Computers and Mathematics with Applications 150 (2023) 54–69

Contents lists available at ScienceDirect

Computers and Mathematics with Applications

journal homepage: www.elsevier.com/locate/camwa

Hamiltonian-preserving schemes for the two-dimensional fractional nonlinear Schrödinger wave equations

Yang Liu, Maohua Ran *, Li Zhang

School of Mathematical Sciences and V.C. & V.R. Key Lab of Sichuan Province, Sichuan Normal University, Chengdu 610068, China

ARTICLE INFO

Keywords:
Structure-preserving method
Fractional Schrödinger wave equation
Hamiltonian structure
Averaged vector field method
Fourier pseudo-spectral method

ABSTRACT

The focus of this paper is to construct structure-preserving numerical methods for the fractional nonlinear Schrödinger wave equations in two dimensions. We first develop the Hamiltonian structure of the studied problem by virtue of the variational principle of the functional with fractional Laplacian. A fully-discrete numerical scheme is then proposed by applying the partitioned averaged vector field plus method and the Fourier pseudo-spectral method to the resulting Hamiltonian system. The obtained fully-discrete scheme is proved to be energy-preserving and mass-preserving in discrete sense. For comparison, more numerical methods are also listed. Finally, several numerical experiments are given to support our theoretical results.

1. Introduction

In this paper, we consider the following nonlinear fractional Schrödinger wave equations (NFSWEs)

$$u_{tt} + (-\Delta)^{\alpha/2}u + \mathrm{i}\kappa u_t + \beta|u|^2u = 0, \quad \boldsymbol{x} \in \Omega, t \in (0,T] \tag{1.1}$$

with the initial conditions

$$u(\boldsymbol{x},0) = u_0(\boldsymbol{x}), \quad u_t(\boldsymbol{x},0) = u_1(\boldsymbol{x}), \tag{1.2}$$

and the boundary conditions with periods of $2L$, where $\mathrm{i} = \sqrt{-1}, 1 < \alpha \le 2, \boldsymbol{x} \in \Omega \subset \mathbb{R}^d (d = 1,2), \kappa$ and $\beta > 0$ are both real constants, $u(\boldsymbol{x},t)$ is unknown complex valued function, $u_0(\boldsymbol{x})$ and $u_1(\boldsymbol{x})$ are known smooth functions. The fractional Laplacian can be given by the Fourier transform as

$$(-\Delta)^{\frac{\alpha}{2}}u(\boldsymbol{x},t) = \mathcal{F}^{-1}\left[|\boldsymbol{\xi}|^{\alpha}\mathcal{F}(u(\boldsymbol{\xi},t))\right], \tag{1.3}$$

where $\mathcal{F}$ is the Fourier transform and $\mathcal{F}^{-1}$ denotes its inverse, see [1]. In particular, the fractional Laplacian operator is equivalent to the Riesz fractional derivative in one dimension [2,3], and it will degenerate to the classical Laplacian operator when $\alpha = 2$, and the corresponding integer order classical problem has been studied relatively well, see e.g., [4–7].

The studied problem arises from a variety of physical applications, such as the nonrelativistic limit of the Klein-Gordon equation [8,9], the Langmuir wave envelope approximation in plasma [10], and the modulated planar pulse approximation of the sine-Gordon equation for light bullets [11,12]. It can be regarded as a generalization of the integer order Schrödinger equations, and can be derived by extending the Feynman path integral to the Lévy one, see [13,14].

Like many other differential models based on physical scenario, the studied problem (1.1)-(1.2) with periodic boundary conditions possesses the mass and energy conservation laws as follows

$$G(t) = G(0), \quad E(t) = E(0), \quad 0 < t \le T, \tag{1.4}$$

where the mass

$$G(t) = \kappa\|u(\cdot,t)\|^2 + 2\,\mathrm{Im}\left(u_t, u\right), \tag{1.5}$$

and the energy

$$E(t) = \frac{1}{2}\left(\|u_t(\cdot,t)\|^2 + \left\|(-\Delta)^{\frac{\alpha}{4}}u(\cdot,t)\right\|^2 + \frac{\beta}{2}\|u(\cdot,t)\|_{L^4}^4\right). \tag{1.6}$$

It can be obtained by taking inner product of (1.1) with u and u_t respectively, and noticing that

$$\int_{\Omega}(-\Delta)^{\frac{\alpha}{2}}u(\boldsymbol{x},t)\bar{u}(\boldsymbol{x},t)d\boldsymbol{x} = \int_{\Omega}(-\Delta)^{\frac{\alpha}{4}}u(\boldsymbol{x},t)(-\Delta)^{\frac{\alpha}{4}}\bar{u}(\boldsymbol{x},t)d\boldsymbol{x}. \tag{1.7}$$

In view of this, we want to construct numerical methods that preserve these physical invariants. This is because the capacity to preserve some invariant properties of the original differential equation has become a criterion for evaluating the success of a numerical simulation

* Corresponding author at: School of Mathematical Sciences and V.C. & V.R. Key Lab of Sichuan Province, Sichuan Normal University, Chengdu 610068, China.
E-mail addresses: liuyang@stu.sicnu.edu.cn (Y. Liu), maohuaran@163.com (M. Ran).

https://doi.org/10.1016/j.camwa.2023.09.011
Received 3 May 2023; Received in revised form 23 August 2023; Accepted 11 September 2023
Available online 27 September 2023

in some fields, see [15]. Also, Kang Feng said "A basic idea behind the design of numerical schemes is that they can preserve the properties of the original problems as much as possible". In fact, over the last 10 years, many researchers have paid attention to this topic. For example, Wang and Xiao [16] firstly presented a Crank-Nicolson difference scheme which conserves the discrete mass for the coupled nonlinear fractional Schrödinger equations, and then, in [17], they further proposed a linearly implicit scheme which conserves a modified discrete mass and energy. Ran and Zhang [18] proposed an implicit difference scheme and linear difference scheme which preserves the original and modified mass and energy respectively for the strongly coupled nonlinear fractional Schrödinger equations. Wang and Huang [19,20] derived an energy and mass conservative Crank-Nicolson difference scheme and linear difference scheme for the single cubic fractional Schrödinger equations. Wang et al. [21] presented a split-step spectral Galerkin method for the two-dimensional nonlinear space-fractional Schrödinger equation, which only conserves the discrete mass. In terms of the model problem (1.1)-(1.2), Ran and Zhang [22] first developed a three-level linearly implicit difference scheme which preserves a modified discrete mass and energy well. Li and Zhao [23] considered a conservative strategy by combining the Crank-Nicolson method with the Galerkin finite element method, and a fast Krylov subspace solver with suitable circulant preconditioner is designed to save computational cost. Cheng and Qin [24] developed a linearly-implicit conservative numerical scheme based on the scalar auxiliary variable (SAV) method, which only preserves a modified energy, not mass. Hu et al. [25] proposed three energy-preserving spectral Galerkin methods by applying Crank-Nicolson, SAV and exponential-SAV(ESAV) methods in time respectively. Zhang and Ran [26] proposed and analyzed the higher order energy-preserving difference scheme based on triangular-SAV(T-SAV) approach.

However, existing work has focused almost exclusively on the one-dimensional case, and these proposed methods only preserve energy, or even modified energy. This leads us to develop more effective methods that can preserve the original energy and mass for solving multi-dimensional problems. Noticing that the averaged vector field (AVF) method can preserve the energy for Hamiltonian systems [27,28]. Moreover, the partitioned averaged vector field (PAVF) methods recently proposed that can preserve more conservative property besides the conventional energy, and it has been used to construct conservative schemes for Hamiltonian ordinary differential equations, see [29]. These research foundations make it possible for us to achieve our goals, and the derivation of the Hamiltonian structure for studied problem (1.1)-(1.2) is the successful key for construction of structure preserving methods.

To our knowledge, there are few works focusing on the Hamiltonian structure of fractional differential equations. Recently, Wang and Huang [30] presented the variational derivative of the functional with fractional Laplacian, and reformulated the one-dimensional fractional nonlinear Schrödinger equation as a Hamiltonian system. Fu and Cai [31] derive the Hamiltonian formulation of the two-dimensional fractional Klein-Gordon-Schrödinger equation, and subsequently developing conservative schemes. Based on this, we first derive the Hamiltonian formulation of the two-dimensional NFSWEs (1.1)-(1.2) with periodic boundary conditions, and then successfully construct conservative schemes by combining the partitioned averaged vector field plus (PAVF-P) method and the Fourier pseudo-spectral method.

The remainder of this work is organized as follows. In Section 2, we first investigate the Hamiltonian structure of the two dimensional NFSWEs (1.1)-(1.2) with periodic boundary conditions, and then we derive a semi-discrete conservative system by using the Fourier pseudo-spectral method to approximate the resulting Hamiltonian system in space. In Section 3, we obtain a class of fully-discrete conservative schemes by utilizing the PAVF-P method to discrete the previous space semi-discrete system, and prove the discrete conservation laws. Numerical examples in one and two dimensions are presented in Section 4 to demonstrate the theoretical results. Section 5 presents some conclusions.

2. Hamiltonian structure and space semi-discrete system

2.1. Hamiltonian structure of NFSWEs

It is well-known that Hamiltonian structure is crucial in constructing structure-preserving algorithms for some problems. However, to our knowledge, no researchers have considered the Hamiltonian structure of NFSWEs (1.1)-(1.2). Based on this, here we first reconstruct the Hamiltonian structure of such problem with periodic boundary conditions.

Setting

$$u = p + \mathrm{i}q, u_t = \varphi + \mathrm{i}\psi, \tag{2.1}$$

where p, q, φ, ψ are all real-valued functions. Then, NFSWEs (1.1) can be rewritten as

$$\varphi_t + \mathrm{i}\psi_t + (-\Delta)^{\frac{\alpha}{2}} p + \mathrm{i}(-\Delta)^{\frac{\alpha}{2}} q + \mathrm{i}\kappa\varphi - \kappa\psi + \beta\left(p^2+q^2\right)(p+\mathrm{i}q) = 0. \tag{2.2}$$

Separating the real and imaginary parts from the above equation gives that

$$\begin{aligned} &\varphi_t + (-\Delta)^{\frac{\alpha}{2}} p - \kappa\psi + \beta\left(p^2+q^2\right)p = 0, \\ &\psi_t + (-\Delta)^{\frac{\alpha}{2}} q + \kappa\varphi + \beta\left(p^2+q^2\right)q = 0. \end{aligned} \tag{2.3}$$

Namely, NFSWEs (1.1) can be rewritten as an equivalent coupled system

$$\varphi_t = -(-\Delta)^{\frac{\alpha}{2}} p + \kappa\psi - \beta\left(p^2+q^2\right)p, \tag{2.4}$$

$$\psi_t = -(-\Delta)^{\frac{\alpha}{2}} q - \kappa\varphi - \beta\left(p^2+q^2\right)q, \tag{2.5}$$

$$p_t = \varphi, \tag{2.6}$$

$$q_t = \psi, \tag{2.7}$$

where p, q, φ, ψ subject to the periodic boundary conditions.

In order to get the Hamiltonian formulation of NFSWEs (1.1), we introduce two important lemmas.

Lemma 2.1. *[30] For a functional $F[g]$ with the following form*

$$F[g] = \int_\Omega f\left(g(\boldsymbol{x}), (-\Delta)^{\frac{\alpha}{4}} g(\boldsymbol{x})\right) d\boldsymbol{x}, \tag{2.8}$$

where f is smooth function on Ω, the variational derivative of $F[g]$ is given as follows

$$\frac{\delta F}{\delta g} = \frac{\partial f}{\partial g} + (-\Delta)^{\frac{\alpha}{4}} \frac{\partial f}{\partial\left((-\Delta)^{\frac{\alpha}{4}} g\right)}. \tag{2.9}$$

Lemma 2.2. *[31] Given $1 < \alpha \le 2$, then for any real periodic functions $p, q \in L^2(\Omega)$, we have*

$$\int_\Omega (-\Delta)^{\frac{\alpha}{2}} pq\, d\boldsymbol{x} = \int_\Omega (-\Delta)^{\frac{\alpha}{4}} p (-\Delta)^{\frac{\alpha}{4}} q\, d\boldsymbol{x} = \int_\Omega p(-\Delta)^{\frac{\alpha}{2}} q\, d\boldsymbol{x}. \tag{2.10}$$

Based on the above preparation, we can prove the following results.

Theorem 2.3. *Let*

$$\mathcal{G} = \kappa \int_\Omega (p^2+q^2) d\boldsymbol{x} + 2\,\mathrm{Im}\Big(\int_\Omega (\varphi + \mathrm{i}\psi)(p - \mathrm{i}q) d\boldsymbol{x}\Big), \tag{2.11}$$

$$\mathcal{H} = \frac{1}{2}\int_\Omega \left(\left(\varphi^2+\psi^2\right) + \left((-\Delta)^{\frac{\alpha}{4}} p\right)^2 + \left((-\Delta)^{\frac{\alpha}{4}} q\right)^2 + \frac{\beta}{2}(p^2+q^2)^2\right) d\boldsymbol{x}. \tag{2.12}$$

Then the equivalent system (2.4)-(2.7) has the following two conservation laws:

$$\frac{d}{dt}\mathcal{G}=0,\ \frac{d}{dt}\mathcal{H}=0. \tag{2.13}$$

Proof. Computing the inner product of (2.4) and (2.5) with φ and ψ respectively, one immediately gets the first conservation law. Noticing that Lemma 2.2, and taking the inner products of (2.4)-(2.7) with $\varphi_t, \psi_t, p_t, -q_t$ respectively, one can deduce that the second conservation law. This proof is completed. □

Theorem 2.4. *NFSWEs (1.1) can be reorganized into Hamiltonian system*

$$\begin{pmatrix}\varphi_t\\ \psi_t\\ p_t\\ q_t\end{pmatrix}=J\begin{pmatrix}\delta\mathcal{H}/\delta\varphi\\ \delta\mathcal{H}/\delta\psi\\ \delta\mathcal{H}/\delta p\\ \delta\mathcal{H}/\delta q\end{pmatrix}, \tag{2.14}$$

where the Hamilton operator

$$J=\begin{pmatrix}0&\kappa&-1&0\\ -\kappa&0&0&-1\\ 1&0&0&0\\ 0&1&0&0\end{pmatrix}, \tag{2.15}$$

and the energy functional $\mathcal{H}$ is defined in (2.12).

Proof. Noticing that

$$\begin{aligned}(-\Delta)^{\frac{\alpha}{4}}((-\Delta)^{\frac{\alpha}{4}}u(\boldsymbol{x},t))&=\mathcal{F}^{-1}\left[|\boldsymbol{\sigma}|^{\frac{\alpha}{2}}\mathcal{F}(\mathcal{F}^{-1}\left[|\boldsymbol{\sigma}|^{\frac{\alpha}{2}}\mathcal{F}(u(\boldsymbol{\sigma},t))\right])\right]\\ &=\mathcal{F}^{-1}\left[|\boldsymbol{\sigma}|^{\frac{\alpha}{2}}|\boldsymbol{\sigma}|^{\frac{\alpha}{2}}\mathcal{F}(u(\boldsymbol{\sigma},t))\right]\\ &=\mathcal{F}^{-1}\left[|\boldsymbol{\sigma}|^{\alpha}\mathcal{F}(u(\boldsymbol{\sigma},t))\right]\\ &=(-\Delta)^{\frac{\alpha}{2}}u(\boldsymbol{x},t),\end{aligned} \tag{2.16}$$

and applying the fractional variational principle in Lemma 2.1 yields that

$$\frac{\delta\mathcal{H}}{\delta p}=\frac{1}{2}\left(2(-\Delta)^{\frac{\alpha}{2}}p+2\cdot\frac{\beta}{2}\left(p^2+q^2\right)\cdot 2p\right)=(-\Delta)^{\frac{\alpha}{2}}p+\beta\left(p^2+q^2\right)p, \tag{2.17}$$

$$\frac{\delta\mathcal{H}}{\delta q}=\frac{1}{2}\left(2(-\Delta)^{\frac{\alpha}{2}}q+2\cdot\frac{\beta}{2}\left(p^2+q^2\right)\cdot 2q\right)=(-\Delta)^{\frac{\alpha}{2}}q+\beta\left(p^2+q^2\right)q, \tag{2.18}$$

$$\frac{\delta\mathcal{H}}{\delta\varphi}=\varphi, \tag{2.19}$$

$$\frac{\delta\mathcal{H}}{\delta\psi}=\psi. \tag{2.20}$$

This together with the equivalent form (2.4)-(2.7) of NFSWEs (1.1) deduces that

$$\begin{pmatrix}\varphi_t\\ \psi_t\\ p_t\\ q_t\end{pmatrix}=\begin{pmatrix}0&\kappa&-1&0\\ -\kappa&0&0&-1\\ 1&0&0&0\\ 0&1&0&0\end{pmatrix}\begin{pmatrix}\delta\mathcal{H}/\delta\varphi\\ \delta\mathcal{H}/\delta\psi\\ \delta\mathcal{H}/\delta p\\ \delta\mathcal{H}/\delta q\end{pmatrix}. \tag{2.21}$$

This proof is completed. □

2.2. Space semi-discrete system

Considering the periodic boundary conditions, we choose the Fourier pseudo-spectral method for space discretization of NFSWEs (1.1).

Without loss of generality, we set $d=2$. For positive integer M and even positive integers N_x and N_y, denote $\tau=T/M, h_x=2L/N_x, h_y=2L/N_y$. Define $\Omega_h^\tau=\Omega_h\times\Omega_\tau$, where $\Omega_h=\left\{(x_i,y_j)\mid i=0,1,\cdots,N_x-1;\ j=0,1,\cdots,N_y-1\right\}$ and $\Omega_\tau=\left\{t_m\mid t_m=m\tau, 0\le m\le M\right\}$, with $t_m=m\tau, x_i=-L+ih_x$ and $y_j=-L+jh_y$.

For any grid functions u and v defined on Ω_h, we define the discrete inner product and the associated discrete norms as

$$(u,v)=h_xh_y\sum_{i=0}^{N_x-1}\sum_{j=0}^{N_y-1}u_{i,j}v_{i,j},\quad \|u\|=(u,u)^{\frac{1}{2}},\quad \|u\|_\infty=\sup_{(x_i,y_j)\in\Omega_h}\left|u_{i,j}\right|. \tag{2.22}$$

For brevity, we introduce following operators

$$\delta_tU^m=\frac{U^{m+1}-U^m}{\tau},\quad U^{m+\frac{1}{2}}=\frac{U^{m+1}+U^m}{2}, \tag{2.23}$$

where

$$U^m=\left(u_{0,0}^m,\cdots,u_{N_x-1,0}^m,u_{0,1}^m,\cdots,u_{N_x-1,1}^m,\cdots,u_{0,N_y-1}^m,\cdots,u_{N_x-1,N_y-1}^m\right)^T. \tag{2.24}$$

Let $(x_i,y_j)\in\Omega_h$ be the Fourier collocation points. Denote $u_N(x,y)$ is the interpolation polynomial function of $u(x,y)$, then we have

$$u_N(x,y)=\sum_{k_1=-N_x/2}^{N_x/2}\sum_{k_2=-N_y/2}^{N_y/2}\tilde{u}_{k_1,k_2}e^{\mathrm{i}\mu\left(k_1(x+L)+k_2(y+L)\right)}, \tag{2.25}$$

in which $\mu=\pi/L$, and the coefficient

$$\tilde{u}_{k_1,k_2}=\frac{1}{N_xc_{k_1}}\frac{1}{N_yc_{k_2}}\sum_{l_1=0}^{N_x-1}\sum_{l_2=0}^{N_y-1}u(x_{l_1},y_{l_2})e^{-\mathrm{i}\mu\left(k_1(x_{l_1}+L)+k_2(y_{l_2}+L)\right)}, \tag{2.26}$$

where $c_{k_1}=1$ for $|k_1|<N_x/2, c_{k_2}=1$ for $|k_2|<N_y/2, c_{k_1}=2$ for $k_1=\pm N_x/2$, and $c_{k_2}=2$ for $k_2=\pm N_y/2$. As a result, the fractional Laplacian $(-\Delta)^{\frac{\alpha}{2}}u(x,y)$ can be approximated by

$$\begin{aligned}(-\Delta)^{\frac{\alpha}{2}}u_N(x,y)=&\sum_{k_1=-N_x/2}^{N_x/2}\sum_{k_2=-N_y/2}^{N_y/2}\left|\left(k_1\mu\right)^2+\left(k_2\mu\right)^2\right|^{\frac{\alpha}{2}}\\ &\times\tilde{u}_{k_1,k_2}e^{\mathrm{i}\mu\left(k_1(x+L)+k_2(y+L)\right)}.\end{aligned} \tag{2.27}$$

Inserting (2.26) into (2.27), and considering the resulting equation at the point (x_i,y_j) gives that

$$\begin{aligned}&(-\Delta)^{\frac{\alpha}{2}}u_N\left(x_i,y_j\right)\\ &=\sum_{l_1=0}^{N_x-1}\sum_{l_2=0}^{N_y-1}u(x_{l_1},y_{l_2})\left(\sum_{k_1=-N_x/2}^{N_x/2}\sum_{k_2=-N_y/2}^{N_y/2}\frac{1}{N_xc_{k_1}}\frac{1}{N_yc_{k_2}}\left|\mu^2\cdot\mathbf{k}^2\right|^{\frac{\alpha}{2}}\right.\\ &\left.\times e^{\mathrm{i}\mu\left(k_1\left(x_i-x_{l_1}\right)+k_2\left(y_j-y_{l_2}\right)\right)}\right)\\ &=(D^\alpha U)_{i+jN_x},\end{aligned} \tag{2.28}$$

where $\mu^2\cdot\mathbf{k}^2=\mu^2\left(k_1^2+k_2^2\right)$, D^α is spectral symmetric differential matrix with the elements

$$\begin{aligned}(D^\alpha)_{i+jN_x,l_1+l_2N_x}=&\sum_{l_1=0}^{N_x-1}\sum_{l_2=0}^{N_y-1}\frac{1}{N_xc_{k_1}}\frac{1}{N_yc_{k_2}}\left|\mu^2\cdot\mathbf{k}^2\right|^{\frac{\alpha}{2}}\\ &\times e^{\mathrm{i}\mu\left(k_1\left(x_i-x_{l_1}\right)+k_2\left(y_j-y_{l_2}\right)\right)}.\end{aligned} \tag{2.29}$$

Applying the Fourier pseudo-spectral method to approximate the previous equivalent system (2.4)-(2.7) in space gives the space semi-discrete system as follows

$$\Phi_t=D^\alpha P+\kappa\Psi-\beta\left(P^2+Q^2\right)\cdot P, \tag{2.30}$$

$$\Psi_t=D^\alpha Q-\kappa\Phi-\beta\left(P^2+Q^2\right)\cdot Q, \tag{2.31}$$

$$P_t=\Phi, \tag{2.32}$$

$$Q_t=\Psi, \tag{2.33}$$

where $P^2 = P \cdot P$, and $\cdot$ means the point multiplication between vectors.

Let

$$Y = \left(\Phi^T, \Psi^T, P^T, Q^T\right), \tag{2.34}$$

then the above semi-discrete system can be rewritten in a canonical Hamiltonian form as

$$\frac{dY}{dt} = f(Y) = S\nabla H(Y), \tag{2.35}$$

where the Hamiltonian energy is defined by

$$H(Y) = \frac{1}{2}\left((\Phi^T\Phi + \Psi^T\Psi) - P^T D^\alpha P - Q^T D^\alpha Q + \frac{\beta}{2}(P^2+Q^2)^T(P^2+Q^2)\right), \tag{2.36}$$

and S is a skew symmetric matrix with the following form

$$S = \begin{pmatrix} 0 & \kappa I & -I & 0 \\ -\kappa I & 0 & 0 & -I \\ I & 0 & 0 & 0 \\ 0 & I & 0 & 0 \end{pmatrix}. \tag{2.37}$$

Also, we define the mass

$$G(Y) = \kappa\|P\|^2 + \kappa\|Q\|^2 + 2\Psi^T P - 2\Phi^T Q. \tag{2.38}$$

Then we have the following theorem.

Theorem 2.5. *The semi-discrete system (2.30)-(2.33) has the mass and energy conservation laws:*

$$\frac{dG(Y)}{dt} = 0, \quad \frac{dH(Y)}{dt} = 0. \tag{2.39}$$

Proof. According to (2.38), one can derive that

$$\begin{aligned}\frac{dG(Y)}{dt} &= 2h_x h_y\left(\kappa P^T P_t + \kappa Q^T Q_t + \Psi_t^T P + \Psi^T P_t - \Phi_t^T Q - \Phi^T Q_t\right)\\ &= 2h_x h_y\left(\kappa P^T\Phi + \kappa Q^T\Psi + P^T D^\alpha Q - \kappa P^T\Phi - \beta P^T\left(P^2+Q^2\right)\cdot Q\right.\\ &\quad \left.+\Psi^T\Phi - Q^T D^\alpha P - \kappa Q^T\Psi + \beta Q^T\left(P^2+Q^2\right)\cdot P - \Phi^T\Psi\right)\\ &= 0.\end{aligned} \tag{2.40}$$

Based on the skew symmetric of the matrix S, it follows from (2.35) that

$$\frac{dH(Y)}{dt} = \nabla H(Y)^T f(Y) = \nabla H(Y)^T S\nabla H(Y) = 0. \tag{2.41}$$

This proof is completed. □

3. Structure-preserving numerical methods

3.1. PAVF-P scheme

For NFSWEs (1.1), there are many structure-preserving methods, but most of these methods only preserve modified energy or mass, see [23,25]. This inspired us to construct numerical methods that not only preserve the original energy, but also preserve original mass. Based on the Hamiltonian system (2.35) established above, here we apply the partitioned averaged vector field (PAVF) method developed in [29] to construct structure-preserving methods for NFSWEs (1.1) because the PAVF method preserves not only traditional energy, but possibly other conservation properties.

Considering the Hamiltonian system (2.35), and applying the PAVF method, we can obtain the fully-discrete scheme for solving NFSWEs (1.1) as follows

$$\begin{aligned}\delta_t\Phi^m = &\int_0^1 \kappa H_\Psi\left(\Phi^{m+1}, \varepsilon\Psi^{m+1} + (1-\varepsilon)\Psi^m, P^m, Q^m\right)\\ &- H_P\left(\Phi^{m+1}, \Psi^{m+1}, \varepsilon P^{m+1} + (1-\varepsilon)P^m, Q^m\right)d\varepsilon,\end{aligned} \tag{3.1}$$

$$\begin{aligned}\delta_t\Psi^m = &\int_0^1 -\kappa H_\Phi\left(\varepsilon\Phi^{m+1} + (1-\varepsilon)\Phi^m, \Psi^m, P^m, Q^m\right)\\ &- H_Q\left(\Phi^{m+1}, \Psi^{m+1}, P^{m+1}, \varepsilon Q^{m+1} + (1-\varepsilon)Q^m\right)d\varepsilon,\end{aligned} \tag{3.2}$$

$$\delta_t P^m = \int_0^1 H_\Phi\left(\varepsilon\Phi^{m+1} + (1-\varepsilon)\Phi^m, \Psi^m, P^m, Q^m\right)d\varepsilon, \tag{3.3}$$

$$\delta_t Q^m = \int_0^1 H_\Psi\left(\Phi^{m+1}, \varepsilon\Psi^{m+1} + (1-\varepsilon)\Psi^m, P^m, Q^m\right)d\varepsilon. \tag{3.4}$$

The above numerical scheme can be further integrated as

$$\begin{aligned}\delta_t\Phi^m = &\kappa\Psi^{m+\frac{1}{2}} + D^\alpha P^{m+\frac{1}{2}} - \frac{\beta}{4}\left((P^{m+1})^3 + (P^m)^2\cdot P^{m+1} + (P^{m+1})^2\cdot P^m\right.\\ &\left.+ (P^m)^3 + 2P^{m+1}\cdot(Q^m)^2 + 2P^m\cdot(Q^m)^2\right),\end{aligned} \tag{3.5}$$

$$\begin{aligned}\delta_t\Psi^m = &-\kappa\Phi^{m+\frac{1}{2}} + D^\alpha Q^{m+\frac{1}{2}} - \frac{\beta}{4}\left((Q^{m+1})^3 + (Q^m)^2\cdot Q^{m+1} + (Q^{m+1})^2\cdot Q^m\right.\\ &\left.+ (Q^m)^3 + 2Q^{m+1}\cdot(P^{m+1})^2 + 2Q^m\cdot(P^{m+1})^2\right),\end{aligned} \tag{3.6}$$

$$\delta_t P^m = \Phi^{m+\frac{1}{2}}, \tag{3.7}$$

$$\delta_t Q^m = \Psi^{m+\frac{1}{2}}. \tag{3.8}$$

The proposed fully-discrete scheme (3.5)-(3.8) will hereafter be called FPAVF (Fourier pseudo-spectral PAVF) scheme. The energy conservation property of the FPAVF scheme can be easily obtained by taking the inner product of (3.5)-(3.6) with $\delta_t P^m$ and $\delta_t Q^m$ respectively. Unfortunately this scheme does not guarantee the conservation of mass, which can be reflected in numerical examples.

The adjoint of the FPAVF scheme (3.5)-(3.8) can be reads as

$$\begin{aligned}\delta_t\Phi^m = &\kappa\Psi^{m+\frac{1}{2}} + D^\alpha P^{m+\frac{1}{2}} - \frac{\beta}{4}\left((P^{m+1})^3 + (P^m)^2\cdot P^{m+1} + (P^{m+1})^2\cdot P^m\right.\\ &\left.+(P^m)^3 + 2P^{m+1}\cdot(Q^{m+1})^2 + 2P^m\cdot(Q^{m+1})^2\right),\end{aligned} \tag{3.9}$$

$$\begin{aligned}\delta_t\Psi^m = &-\kappa\Phi^{m+\frac{1}{2}} + D^\alpha Q^{m+\frac{1}{2}} - \frac{\beta}{4}\left((Q^{m+1})^3 + (Q^m)^2\cdot Q^{m+1} + (Q^{m+1})^2\cdot Q^m\right.\\ &\left.+(Q^m)^3 + 2Q^{m+1}\cdot(P^m)^2 + 2Q^m\cdot(P^m)^2\right),\end{aligned} \tag{3.10}$$

$$\delta_t P^m = \Phi^{m+\frac{1}{2}}, \tag{3.11}$$

$$\delta_t Q^m = \Psi^{m+\frac{1}{2}}. \tag{3.12}$$

Combining the FPAVF scheme (3.5)-(3.8) and the adjoint FPAVF scheme (3.9)-(3.12), the FPAVF-P (Fourier pseudo-spectral PAVF plus) scheme is given by

$$\begin{aligned}\delta_t\Phi^m = &\kappa\Psi^{m+\frac{1}{2}} + D^\alpha P^{m+\frac{1}{2}} - \frac{\beta}{4}\left((P^{m+1})^3 + (P^m)^2\cdot P^{m+1} + (P^{m+1})^2\cdot P^m\right.\\ &+(P^m)^3 + P^{m+1}\cdot(Q^m)^2 + P^m\cdot(Q^m)^2 + P^{m+1}\cdot(Q^{m+1})^2\\ &\left.+ P^m\cdot(Q^{m+1})^2\right),\end{aligned} \tag{3.13}$$

$$\begin{aligned}\delta_t\Psi^m = &-\kappa\Phi^{m+\frac{1}{2}} + D^\alpha Q^{m+\frac{1}{2}} - \frac{\beta}{4}\left((Q^{m+1})^3 + (Q^m)^2\cdot Q^{m+1} + (Q^{m+1})^2\cdot Q^m\right.\\ &+(Q^m)^3 + Q^{m+1}\cdot(P^{m+1})^2 + Q^m\cdot(P^{m+1})^2 + Q^{m+1}\cdot(P^m)^2\\ &\left.+ Q^m\cdot(P^m)^2\right),\end{aligned} \tag{3.14}$$

$$\delta_t P^m = \Phi^{m+\frac{1}{2}}, \tag{3.15}$$

$$\delta_t Q^m = \Psi^{m+\frac{1}{2}}. \tag{3.16}$$

3.2. Discrete conservation laws

Theorem 3.1. *The FPAVF-P scheme (3.13)-(3.16) has the following properties of energy-preserving and mass-preserving in discrete sense:*

$$G^{m+1} = G^m, \quad H^{m+1} = H^m, \quad 0 \le m \le M-1, \tag{3.17}$$

where the discrete mass is defined as

$$G^m = \kappa\|P^m\|^2 + \kappa\|Q^m\|^2 + 2\left(\Psi^m\right)^T P^m - 2\left(\Phi^m\right)^T Q^m, \tag{3.18}$$

and the discrete energy has the form

$$H^m = \frac{1}{2}[((\Phi^m)^T\Phi^m + (\Psi^m)^T\Psi^m) - ((P^m)^T D^\alpha P^m + (Q^m)^T D^\alpha Q^m) + \frac{\beta}{2}((P^m)^2 + (Q^m)^2)^T((P^m)^2 + (Q^m)^2)]. \tag{3.19}$$

Proof. Taking the inner product of (3.13) with $Q^{m+1} + Q^m$ yields that

$$\begin{aligned}&(Q^{m+1} + Q^m)^T\delta_t\Phi^m\\ &= (Q^{m+1} + Q^m)^T\kappa\Psi^{m+\frac{1}{2}} + (Q^{m+1} + Q^m)^T D^\alpha P^{m+\frac{1}{2}}\\ &\quad - (Q^{m+1} + Q^m)^T\frac{\beta}{4}\left((P^{m+1})^3 + (P^m)^2\cdot P^{m+1} + (P^{m+1})^2\cdot P^m\right.\\ &\quad \left.+(P^m)^3 + P^{m+1}\cdot(Q^m)^2 + P^m\cdot(Q^m)^2 + P^{m+1}\cdot(Q^{m+1})^2 + P^m\cdot(Q^{m+1})^2\right).\end{aligned} \tag{3.20}$$

Similarly, taking the inner product of (3.14) with $P^{m+1} + P^m$ gives that

$$\begin{aligned}&(P^{m+1} + P^m)^T\delta_t\Psi^m\\ &= -(P^{m+1} + P^m)^T\kappa\Phi^{m+\frac{1}{2}} + (P^{m+1} + P^m)^T D^\alpha Q^{m+\frac{1}{2}}\\ &\quad - (P^{m+1} + P^m)^T\frac{\beta}{4}\left((Q^{m+1})^3 + (Q^m)^2\cdot Q^{m+1} + (Q^{m+1})^2\cdot Q^m\right.\\ &\quad \left.+(Q^m)^3 + Q^{m+1}\cdot(P^{m+1})^2 + Q^m\cdot(P^{m+1})^2 + Q^{m+1}\cdot(P^m)^2 + Q^m\cdot(P^m)^2\right)\end{aligned} \tag{3.21}$$

Subtracting (3.21) from (3.20) deduces that

$$\begin{aligned}&(Q^{m+1} + Q^m)^T\delta_t\Phi^m - (P^{m+1} + P^m)^T\delta_t\Psi^m\\ &= (Q^{m+1} + Q^m)^T\kappa\Psi^{m+\frac{1}{2}} + (P^{m+1} + P^m)^T\kappa\Phi^{m+\frac{1}{2}}.\end{aligned} \tag{3.22}$$

Noticing that

$$\delta_t P^m = \Phi^{m+\frac{1}{2}},\ \delta_t Q^m = \Psi^{m+\frac{1}{2}},$$

one gets that

$$\begin{aligned}&(Q^{m+1} + Q^m)^T\delta_t\Phi^m - (P^{m+1} + P^m)^T\delta_t\Psi^m\\ &= (Q^{m+1} + Q^m)^T\kappa\delta_t Q^m + (P^{m+1} + P^m)^T\kappa\delta_t P^m.\end{aligned} \tag{3.23}$$

That is,

$$\begin{aligned}&(Q^{m+1} + Q^m)^T(\Phi^{m+1} - \Phi^m) - (P^{m+1} + P^m)^T(\Psi^{m+1} - \Psi^m)\\ &= \kappa(\|Q^{m+1}\|^2 - \|Q^m\|^2) + \kappa(\|P^{m+1}\|^2 - \|P^m\|^2).\end{aligned} \tag{3.24}$$

Cross-multiplying (3.15) and (3.16) yields that

$$\begin{aligned}&((Q^{m+1})^T\Phi^{m+1} - (P^{m+1})^T\Psi^{m+1}) - ((Q^m)^T\Phi^m - (P^m)^T\Psi^m)\\ &= ((Q^m)^T\Phi^{m+1} - (P^m)^T\Psi^{m+1}) - ((Q^{m+1})^T\Phi^m - (P^{m+1})^T\Psi^m).\end{aligned} \tag{3.25}$$

Substituting (3.25) into (3.24), one obtains

$$\begin{aligned}&\kappa\|P^{m+1}\|^2 + \kappa\|Q^{m+1}\|^2 + 2(P^{m+1})^T\Psi^{m+1} - 2(Q^{m+1})^T\Phi^{m+1}\\ &= \kappa\|P^m\|^2 + \kappa\|Q^m\|^2 + 2(P^m)^T\Psi^m - 2(Q^m)^T\Phi^m,\end{aligned} \tag{3.26}$$

which implies that

$$G^{m+1} = G^m. \tag{3.27}$$

Similarly, by taking the discrete inner products of (3.13), (3.14) with $\delta_t P^m$ and $\delta_t Q^m$ respectively, and summing them together, one can obtain the energy conservation law

$$H^{m+1} = H^m. \tag{3.28}$$

This proof is completed. □

3.3. Other numerical methods

For comparison, we also give the following two second-order AVF schemes for NFSWEs (1.1).

- The FAVF (Fourier pseudo-spectral AVF) scheme

$$\begin{aligned}\delta_t\Phi &= D^\alpha P^{m+\frac{1}{2}} + \kappa\Psi^{m+\frac{1}{2}} - \frac{\beta}{12}\left(3(P^{m+1})^3 - 5(P^{m+1})^2\cdot P^m\right.\\ &\quad - 5(P^m)^2\cdot P^{m+1} + 19(P^m)^3 - 6Q^{m+1}\cdot Q^m\cdot P^m\\ &\quad + 2Q^{m+1}\cdot Q^m\cdot P^{m+1}\\ &\quad + 3(Q^{m+1})^2\cdot P^{m+1} + (Q^m)^2\cdot P^{m+1} - 7(Q^{m+1})^2\cdot P^m\\ &\quad \left.+19(Q^m)^2\cdot P^m\right),\end{aligned} \tag{3.29}$$

$$\begin{aligned}\delta_t\Psi &= D^\alpha Q^{m+\frac{1}{2}} - \kappa\Phi^{m+\frac{1}{2}} - \frac{\beta}{12}\left(3(Q^{m+1})^3 - 5(Q^{m+1})^2\cdot Q^m\right.\\ &\quad - 5(Q^m)^2\cdot Q^{m+1} + 19(Q^m)^3 - 6P^{m+1}\cdot P^m\cdot Q^m\\ &\quad + 2P^{m+1}\cdot P^m\cdot Q^{m+1}\\ &\quad + 3(P^{m+1})^2\cdot Q^{m+1} + (P^m)^2\cdot Q^{m+1} - 7(P^{m+1})^2\cdot Q^m\\ &\quad \left.+ 19(P^m)^2\cdot Q^m\right),\end{aligned} \tag{3.30}$$

$$\delta_t P = \Phi^{m+\frac{1}{2}}, \tag{3.31}$$

$$\delta_t Q = \Psi^{m+\frac{1}{2}}. \tag{3.32}$$

- The FPAVF-C (Fourier pseudo-spectral PAVF composition) scheme

$$\begin{aligned}\frac{1}{\tau}(\Phi^* - \Phi^m) &= \frac{1}{2}\kappa(\Psi^* + \Psi^m) + \frac{1}{2}D^\alpha(P^* + P^m)\\ &\quad - \frac{\beta}{4}\left((P^*)^3 + (P^m)^2\cdot P^* + (P^*)^2\cdot P^m\right.\\ &\quad \left.+(P^m)^3 + 2P^*\cdot(Q^m)^2 + 2P^m\cdot(Q^m)^2\right),\end{aligned} \tag{3.33}$$

$$\begin{aligned}\frac{1}{\tau}(\Psi^* - \Psi^m) &= -\frac{1}{2}\kappa(\Phi^* + \Phi^m) + \frac{1}{2}D^\alpha(Q^* + Q^m)\\ &\quad - \frac{\beta}{4}\left((Q^*)^3 + (Q^m)^2\cdot Q^* + (Q^*)^2\cdot Q^m\right.\\ &\quad \left.+(Q^m)^3 + 2Q^*\cdot(P^*)^2 + 2Q^m\cdot(P^*)^2\right),\end{aligned} \tag{3.34}$$

$$\frac{1}{\tau}(P^* - P^m) = \frac{1}{2}(\Phi^* + \Phi^m), \tag{3.35}$$

$$\frac{1}{\tau}(Q^* - Q^m) = \frac{1}{2}(\Psi^* + \Psi^m), \tag{3.36}$$

$$\begin{aligned}\frac{1}{\tau}(\Phi^{m+1} - \Phi^*) &= \frac{1}{2}\kappa(\Psi^{m+1} + \Psi^*) + \frac{1}{2}D^\alpha P^{m+\frac{1}{2}}\\ &\quad - \frac{\beta}{4}\left((P^{m+1})^3 + (P^*)^2\cdot P^{m+1} + (P^{m+1})^2\cdot P^*\right.\\ &\quad \left.+(P^*)^3 + 2P^{m+1}\cdot(Q^{m+1})^2 + 2P^*\cdot(Q^{m+1})^2\right),\end{aligned} \tag{3.37}$$

$$\begin{aligned}\frac{1}{\tau}(\Psi^{m+1} - \Psi^*) &= -\frac{1}{2}\kappa(\Phi^{m+1} + \Phi^*) + \frac{1}{2}D^\alpha Q^{m+\frac{1}{2}}\\ &\quad - \frac{\beta}{4}\left((Q^{m+1})^3 + (Q^*)^2\cdot Q^{m+1} + (Q^{m+1})^2\cdot Q^*\right.\\ &\quad \left.+(Q^*)^3 + 2Q^{m+1}\cdot(P^*)^2 + 2Q^*\cdot(P^*)^2\right),\end{aligned} \tag{3.38}$$

$$\frac{1}{\tau}(P^{m+1} - P^*) = \frac{1}{2}(\Phi^{m+1} + \Phi^*), \tag{3.39}$$

$$\frac{1}{\tau}(Q^{m+1} - Q^*) = \frac{1}{2}(\Psi^{m+1} + \Psi^*), \tag{3.40}$$

where Φ^*, Ψ^*, P^*, Q^* denote the intermediary variables obtained iteratively from the preceding layer and used as inputs to calculate the variables of the subsequent layer.

Remark 3.2. Similar to FPAVF-P scheme (3.13)-(3.16), it is easy to prove that the above FPAVF scheme (3.5)-(3.8), FAVF scheme (3.29)-(3.32) and the FPAVF-C scheme (3.33)-(3.40) all preserve the original energy but not the original mass, and the discrete energy has the same form defined in (3.19).

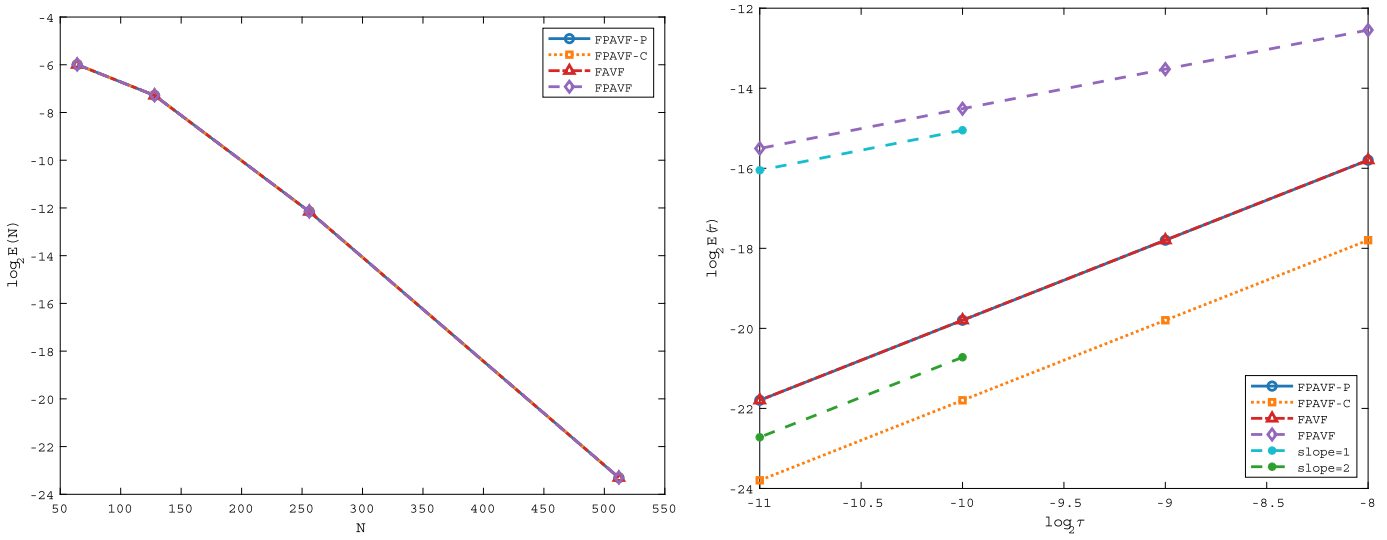

(a) $\tau = 1/1000$ (b) $N = 128$

Fig. 1. Convergence orders of four schemes for Example 4.1 with $\alpha = 1.5$.

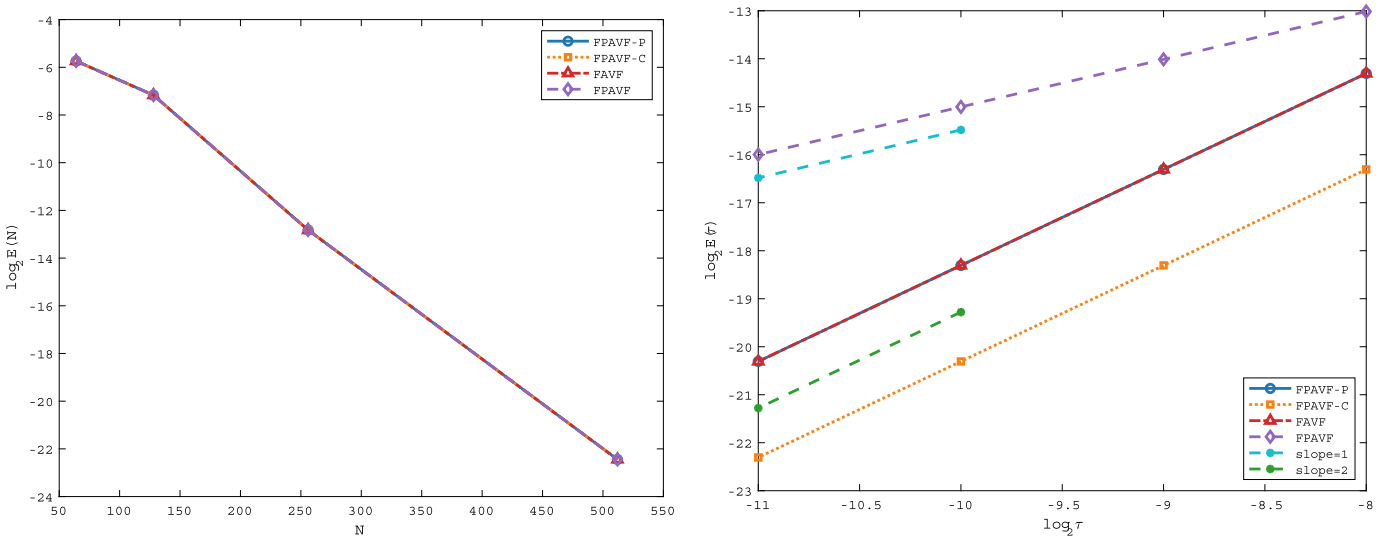

(a) $\tau = 1/1000$ (b) $N = 128$

Fig. 2. Convergence orders of four schemes for Example 4.1 with $\alpha = 2.0$.

Remark 3.3. It is worth emphasizing that the other existing methods for solving NFSWEs (1.1)-(1.2) only preserve modified energy and (or) modified mass. For example, the SAV method [24] only preserves modified energy, three-level linearly implicit difference scheme [22] preserves modified energy and mass. However the proposed FPAVF-P scheme (3.13)-(3.16) preserves both original mass and energy in discrete sense. This is one of the main contributions. Also the FPAVF-P scheme (3.13)-(3.16) has second-order accuracy in time and spectral accuracy in space.

4. Numerical examples

To support and verify previous theoretical results, some numerical examples are provided in this section. In our calculation, a fast solver method based on the fast Fourier transformation (FFT) methodology is employed, which can reduce memory requirements and computational complexity.

To obtain numerical errors, we utilize the following error functions

$$E(\tau) = \left\| U_N^M - U_N^{2M} \right\|_\infty, \quad E(N) = \left\| U_N^M - U_{2N}^M \right\|_\infty, \tag{4.1}$$

where

$$\left\| U_N^M - U_N^{2M} \right\|_\infty = \left\| U\left(\frac{T}{M}, \frac{L}{N}\right) - U\left(\frac{T}{2M}, \frac{L}{N}\right) \right\|_\infty,$$

$$\left\| U_N^M - U_{2N}^M \right\|_\infty = \left\| U\left(\frac{T}{M}, \frac{L}{N}\right) - U\left(\frac{T}{M}, \frac{L}{2N}\right) \right\|_\infty,$$

and the convergence orders in time and space on two successive time step sizes τ and $\tau/2$ and two successive polynomial degrees N and $2N$ are calculated by

$$\text{order} = \begin{cases} \log_2[E(\tau)/E(\tau/2)], \text{ in time} \\ \log_2[E(N)/E(2N)], \text{ in space.} \end{cases} \tag{4.2}$$

In order to depict the conservation performance, the relative errors of energy and mass are calculated by

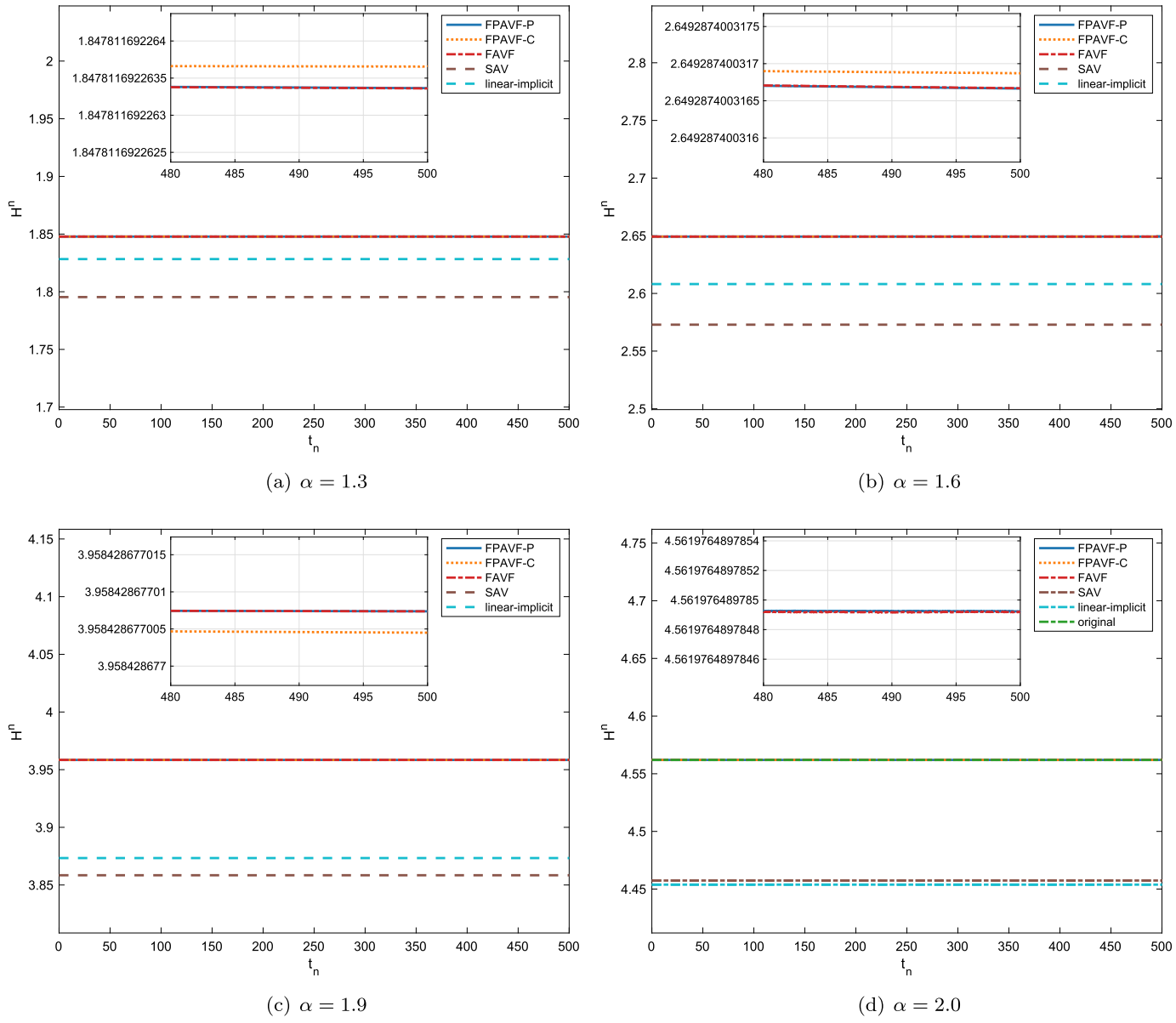

(a) $\alpha = 1.3$ (b) $\alpha = 1.6$

(c) $\alpha = 1.9$ (d) $\alpha = 2.0$

Fig. 3. Discrete energy for different α in Example 4.1 with $N = 512$ and $\tau = 0.01$.

$$RH^n = \left|\left(H^n - H^0\right)/H^0\right|, \quad RG^n = \left|\left(G^n - G^0\right)/G^0\right|, \tag{4.3}$$

where H^n, G^n denote the discrete energy and mass at t_n respectively.

Example 4.1. Firstly, we consider the 1D NFSWEs (1.1)-(1.2) as

$$u_{tt} + (-\Delta)^{\alpha/2}u + \mathrm{i}u_t + |u|^2 u = 0, \quad (x,t) \in \Omega \times [0,T], \tag{4.4}$$

with $u(x,0) = (1+\mathrm{i})xe^{-10(1-x)^2}$ and $u_t(x,0) = 0$.

Based on the conservation laws in discrete sense given in (3.17), one has $G^n \equiv G^0$ and $H^n \equiv H^0$, and G^0, H^0 only depend on the given initial value functions $u(x,0)$ and $u_t(x,0)$. It is not difficult to verify that the initial value function $u(x,0)$ exponentially decays to zero along x away from $x = 1$. It means that the initial value function could be negligible outside a bounded interval Ω. Here, we take $\Omega = (-25, 25)$. Based on the conservation laws in continuous case defined by (1.4), using the Gaussian numerical integration, we immediately have the original mass $G(0) = 0.812482096009503$ for any α, and the original energy $E(0) = 4.56197648980619$ for $\alpha = 2$.

We first compute the convergence orders of above four schemes (the FPAVF-P, FPAVF, FAVF and FPAVF-C schemes) for $T = 1$ with respect to $\alpha = 1.5$ and $\alpha = 2.0$ respectively, see Figs. 1-2. It is easy to find that the four schemes all have spectral accuracy in space, and the FPAVF scheme exhibits first-order accuracy in time while other schemes exhibit second-order accuracy.

Now we focus on the conservation performance of the existing methods. The evolution of the discrete energy over a long period of time is shown in Fig. 3, which are calculated by $N = 512$ and $\tau = 0.01$ for different α respectively. One can observe that, especially from the results of $\alpha = 2$, the discrete energy computed by the FPAVF-P, FPAVF, FAVF and FPAVF-C schemes are convergent uniformly to the original energy, but the SAV method [24] and three-level linearly implicit difference scheme [22] have poor performance. This phenomenon is consistent with the latter preserves only a modified energy rather than the original energy.

Similarly, the evolution of the discrete mass over a long period of time is shown in Fig. 4. It should be emphasized that the SAV method does not have conservation of mass. One can see that the FPAVF-P scheme is convergent uniformly to the original mass, other methods have relatively poor performance especially the FAVF scheme, and

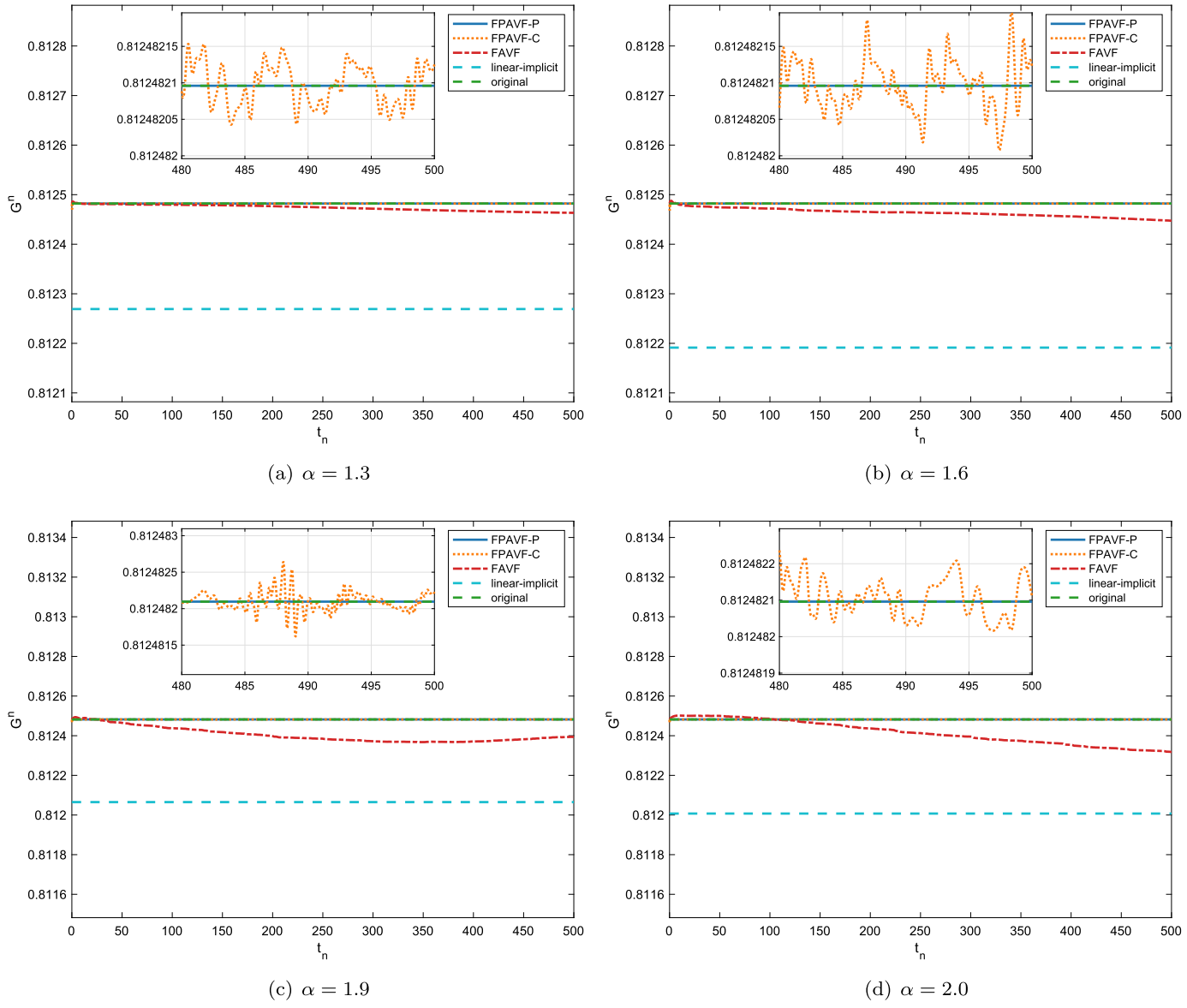

(a) $\alpha = 1.3$ (b) $\alpha = 1.6$

(c) $\alpha = 1.9$ (d) $\alpha = 2.0$

Fig. 4. Discrete mass for different α in Example 4.1 with $N = 512$ and $\tau = 0.01$.

the three-level linearly implicit difference scheme preserves a modified mass. Also the discrete mass based on FPAVF-C scheme shows frequent oscillations on a small scale.

More precisely, the values of discrete energy H^n and discrete mass G^n at different times $t = t_n$ for different α are shown in Tables 1-4, which are obtained by taking $N = 512$ and $\tau = 0.01$. From Table 1, one can see that the proposed four schemes preserve the original energy, but the SAV scheme and linearly implicit difference scheme only preserve a modified energy. Similarly, from Tables 2-4, we observe that the FPAVF-P scheme is convergent uniformly to the original mass, other methods have poor performance and the three-level linearly implicit scheme only conserves modified mass.

Based on the fact that the original energy for $\alpha \neq 2$ is not easy to calculate, we verify the discrete conservation laws from the view of relative error, see Figs. 5-6. Again, these figures show that the FPAVF-P scheme has the best performance in terms of preserves original mass. And with the increase of α, its performance of preserving the original energy will be better. These observations are compatible with our previous theoretical results.

Example 4.2. Now we consider the 2D NFSWEs (1.1)-(1.2) with $\beta = \kappa = 1$ and the initial values

$$u(x,y,0) = \operatorname{sech}\left(x^2+y^2\right), u_t(x,y,0) = \sin(x+y)\operatorname{sech}\left(-2(x^2+y^2)\right), (x,y,t) \in \Omega \times [0,T], \tag{4.5}$$

where $\Omega = [-5,5] \times [-5,5]$.

Similar to one dimensional case, we first compute the convergence orders of the FPAVF-P, FPAVF, FAVF and FPAVF-C schemes for $T = 1$ when $\alpha = 1.5$ and $\alpha = 2.0$ respectively. The change of errors is shown in Figs. 7-8. We can clearly observe that the four schemes all have spectral accuracy in space, and the FPAVF scheme exhibits first-order accuracy while other schemes exhibit second-order accuracy in time.

For comparison the structure preserving ability with the existing methods, we first calculated the original mass and energy. Noticing that the original mass $G(t)$ is independent of α, by using the Gaussian numerical integration, we obtain the original mass $G(0) = 3.14159265323701$ for any α. Similarly, we can get the original energy $E(0) = 3.22697078976648$ for $\alpha = 2$.

Unlike the one-dimensional problem, there is no three-level linear implicit scheme for two-dimensional cases, so below we only compare the performance of the SAV method, and FPAVF-P, FAVF and FPAVF-C schemes proposed in this paper. The evolution of the discrete mass

Table 1
Discrete energy H^n at time $t = t_n$ for Example 4.1 when $\alpha = 2$.

t	FAVF	FPAVF	FPAVF-C	SAV	Linear-Implicit	FPAVF-P
0	4.561976489785	4.561976489785	4.561976489785	4.457414815200	4.453861069486	4.561976489785
10	4.561976489785	4.561976489785	4.561976489785	4.457414815200	4.453861069486	4.561976489785
100	4.561976489785	4.561976489785	4.561976489782	4.457414815197	4.453861069489	4.561976489785
200	4.561976489785	4.561976489785	4.561976489779	4.457414815195	4.453861069492	4.561976489785
300	4.561976489785	4.561976489785	4.561976489776	4.457414815192	4.453861069494	4.561976489785
400	4.561976489785	4.561976489785	4.561976489772	4.457414815190	4.453861069497	4.561976489785
500	4.561976489785	4.561976489785	4.561976489768	4.457414815187	4.453861069500	4.561976489785

Original energy: 4.56197648980619

Table 2
Discrete mass G^n at time $t = t_n$ for Example 4.1 when $\alpha = 1.3$.

t	FAVF	FPAVF	FPAVF-C	Linear-Implicit	FPAVF-P
0	0.812482096011643	0.812486108372853	0.812481093228288	0.812269212105079	0.812482096009232
10	0.812481652913507	0.815448411130831	0.812482228623069	0.812269212105449	0.812482096009234
100	0.812479701090339	0.815337307670638	0.812482081439882	0.812269212105119	0.812482096009236
200	0.812476755660814	0.815352772611703	0.812482091028916	0.812269212105298	0.812482096009256
300	0.812471706145304	0.815369448311709	0.812482102752682	0.812269212105193	0.812482096009262
400	0.812466871593141	0.815375406648485	0.812482112407629	0.812269212105361	0.812482096009263
500	0.812463332390332	0.815391313914498	0.812482125179718	0.812269212105409	0.812482096009261

Original mass: 0.812482096009503

Table 3
Discrete mass G^n at time $t = t_n$ for Example 4.1 when $\alpha = 1.6$.

t	FAVF	FPAVF	FPAVF-C	Linear-Implicit	FPAVF-P
0	0.812482096014526	0.812487932904355	0.812480637459791	0.812191342790779	0.812482096009232
10	0.812479542844467	0.815290680597744	0.812482338980161	0.812191342790869	0.812482096009234
100	0.812471993678066	0.814964610988901	0.812482077830270	0.812191342790519	0.812482096009245
200	0.812465076996841	0.814934135072654	0.812482168949170	0.812191342790438	0.812482096009252
300	0.812461964307183	0.815026734196011	0.812482132284732	0.812191342790211	0.812482096009255
400	0.812456227758388	0.815045189971354	0.812482132454783	0.812191342790067	0.812482096009255
500	0.812447472460440	0.815097180030255	0.812482122664758	0.812191342789578	0.812482096009251

Original mass: 0.812482096009503

Table 4
Discrete mass G^n at time $t = t_n$ for Example 4.1 when $\alpha = 2$.

t	FAVF	FPAVF	FPAVF-C	Linear-Implicit	FPAVF-P
0	0.812482096027426	0.812492566135382	0.812479480708946	0.812007279829162	0.812482096009232
10	0.812501574603936	0.815690689466538	0.812482208549750	0.812007279829185	0.812482096009233
100	0.812485179319911	0.815559529804266	0.812482224295188	0.812007279829068	0.812482096009234
200	0.812436598720768	0.815737264057778	0.812482177481325	0.812007279828906	0.812482096009234
300	0.812395565737519	0.815914179675223	0.812482122649446	0.812007279828999	0.812482096009235
400	0.812353830841431	0.816227202656059	0.812482101787071	0.812007279828969	0.812482096009235
500	0.812317849493374	0.816336221770707	0.812482109657662	0.812007279829037	0.812482096009234

Original mass: 0.812482096009503

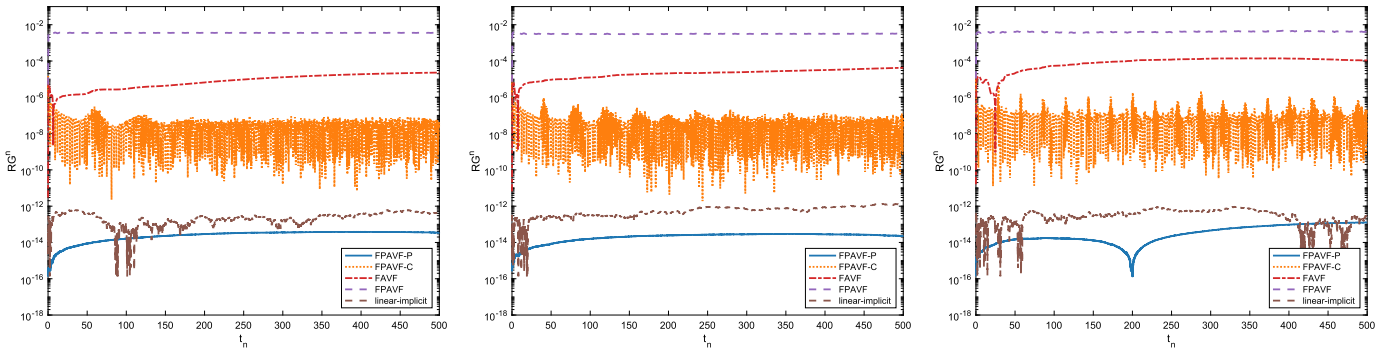

(a) $\alpha = 1.3$ (b) $\alpha = 1.6$ (c) $\alpha = 1.9$

Fig. 5. The relative errors of discrete mass for different α in Example 4.1 with $N = 512$ and $\tau = 0.01$.

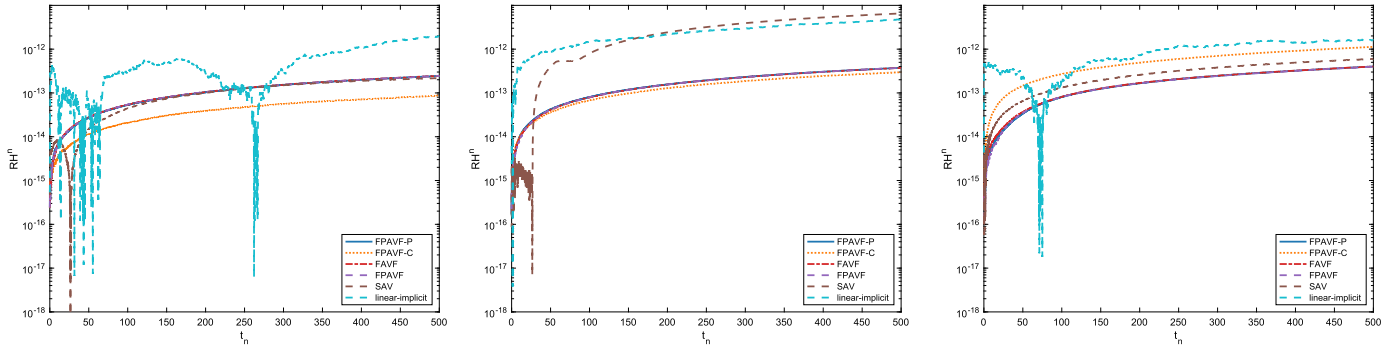

(a) $\alpha = 1.3$ (b) $\alpha = 1.6$ (c) $\alpha = 1.9$

Fig. 6. The relative errors of discrete energy for different α in Example 4.1 with $N = 512$ and $\tau = 0.01$.

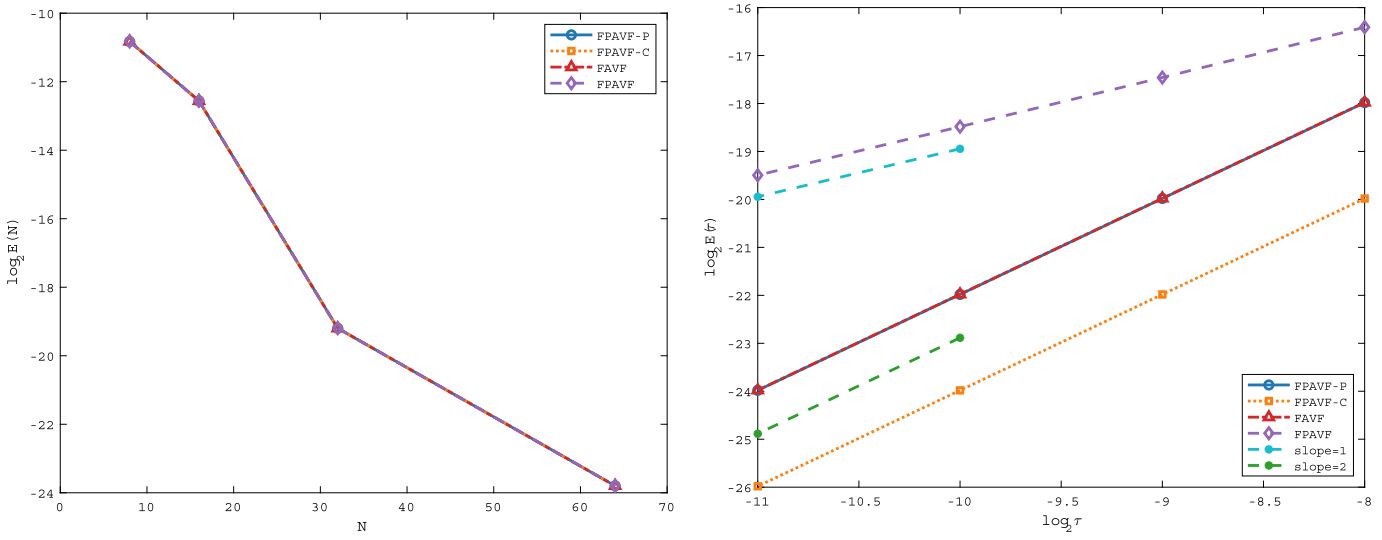

(a) $\tau = 1/1000$ (b) $N = 16$

Fig. 7. Convergence orders of four schemes for Example 4.2 with $\alpha = 1.5$.

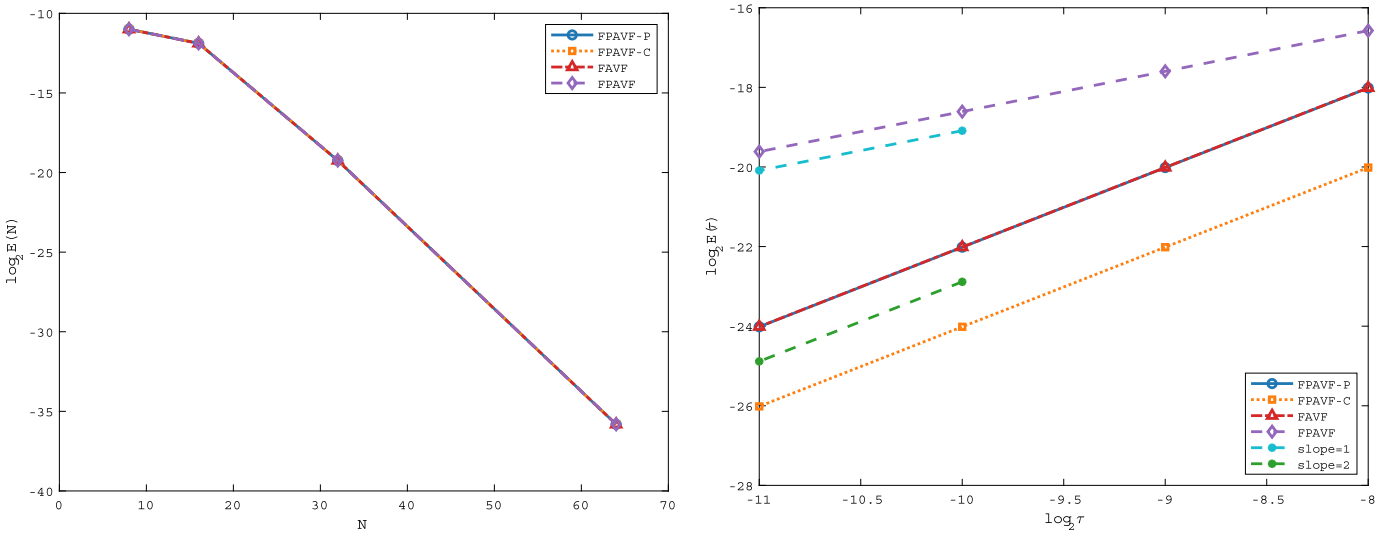

(a) $\tau = 1/1000$ (b) $N = 16$

Fig. 8. Convergence orders of four schemes for Example 4.2 with $\alpha = 2.0$.

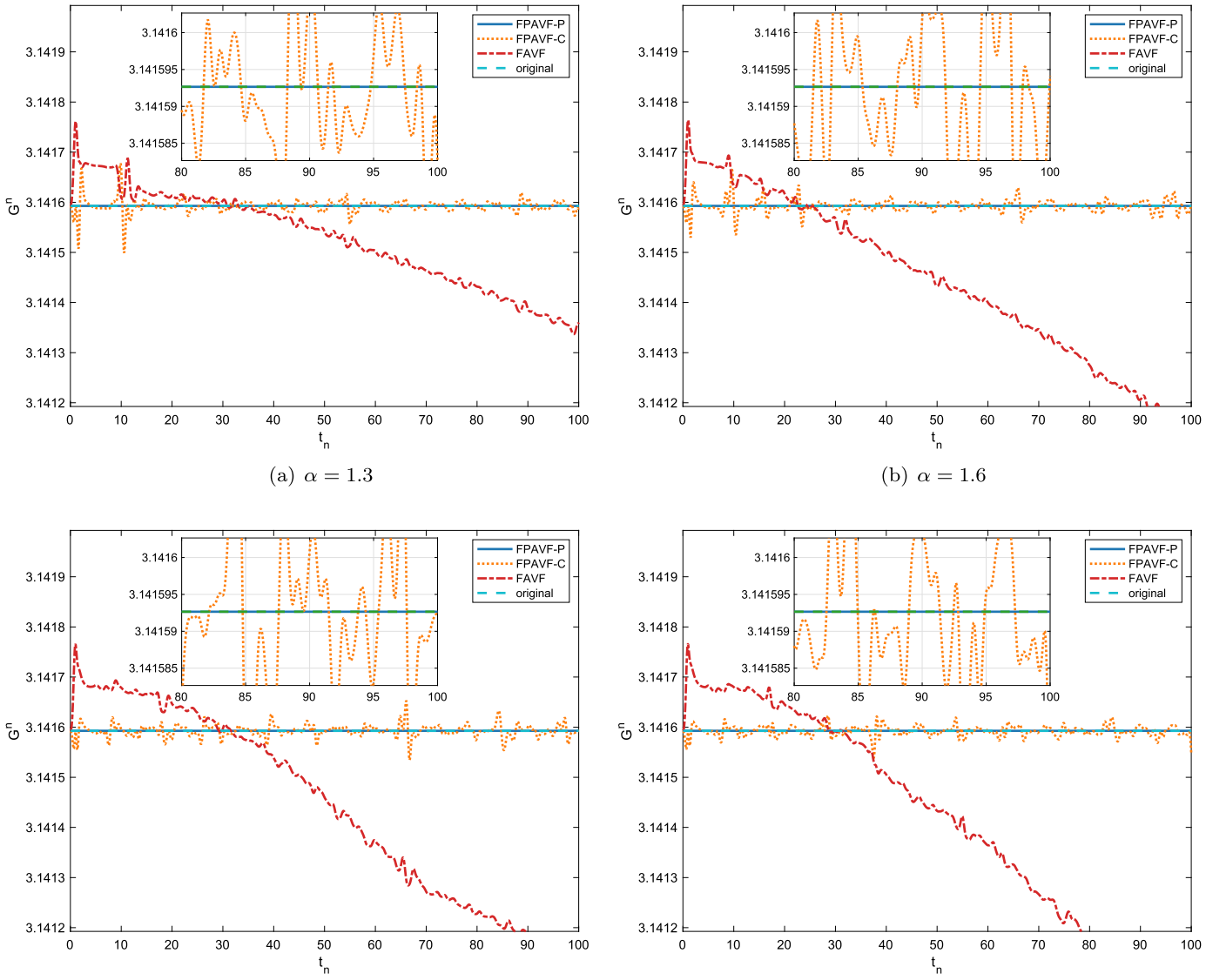

(a) $\alpha = 1.3$ (b) $\alpha = 1.6$

(c) $\alpha = 1.9$ (d) $\alpha = 2.0$

Fig. 9. Discrete mass for different α in Example 4.2 with $N = 64$ and $\tau = 0.01$.

Table 5
Discrete energy H^n at time $t = t_n$ for Example 4.2 when $\alpha = 2$.

t	FAVF	FPAVF	FPAVF-C	SAV	FPAVF-P
0	3.22697078740176	3.22697078740176	3.22697078740173	3.21234862767094	3.22697078740176
10	3.22697078740176	3.22697078740176	3.22697078740168	3.21234862767062	3.22697078740176
20	3.22697078740176	3.22697078740176	3.22697078740172	3.21234862767066	3.22697078740176
40	3.22697078740175	3.22697078740176	3.22697078740182	3.21234862767033	3.22697078740176
60	3.22697078740176	3.22697078740176	3.22697078740191	3.21234862767035	3.22697078740176
80	3.22697078740176	3.22697078740175	3.22697078740199	3.21234862767073	3.22697078740176
100	3.22697078740175	3.22697078740176	3.22697078740207	3.21234862767045	3.22697078740176

Original energy: 3.22697078976648

and discrete energy over a long period of time are shown in Figs. 9-10, which are calculated by $N = 64$ and $\tau = 0.01$ for different α respectively. Also the change of this relative error of discrete mass and energy over time are shown in Figs. 11-12. One can observe that the FPAVF-P scheme is convergent uniformly to the original mass, other three methods have poor performance especially the FAVF scheme and FPAVF scheme (the result with respect to FPAVF scheme is not shown here because it is even worse). And the three schemes proposed in this paper all can preserve the original energy invariance very well, the SAV method only conserves a modified energy. These phenomena once again confirm the correctness of our theoretical results.

A more detailed comparison is shown in Tables 5-8, and we can reach the same conclusion by observing these data.

Finally, we depict the evolution of waves over time t for $\alpha = 1.3, 1.6, 1.99, 2$ in Figs. 13-16 respectively, which are obtained by taking $N = 128$ and $\tau = 0.01$. We can observe that the order α will significantly

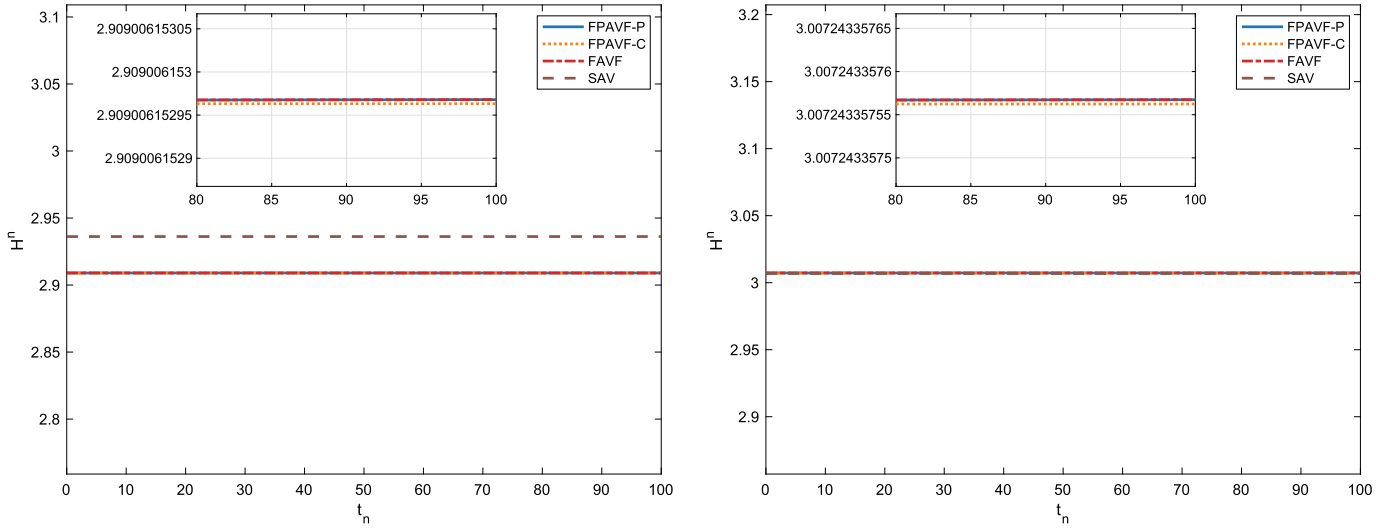

(a) $\alpha = 1.3$ (b) $\alpha = 1.6$

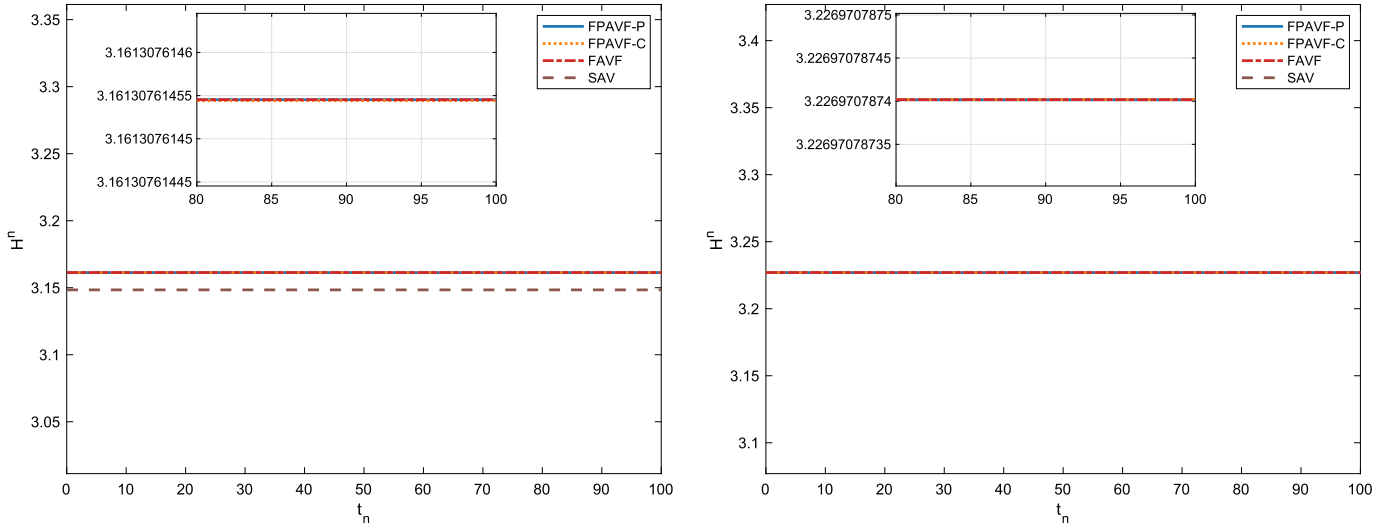

(c) $\alpha = 1.9$ (d) $\alpha = 2.0$

Fig. 10. Discrete energy for different α in Example 4.2 with $N = 64$ and $\tau = 0.01$.

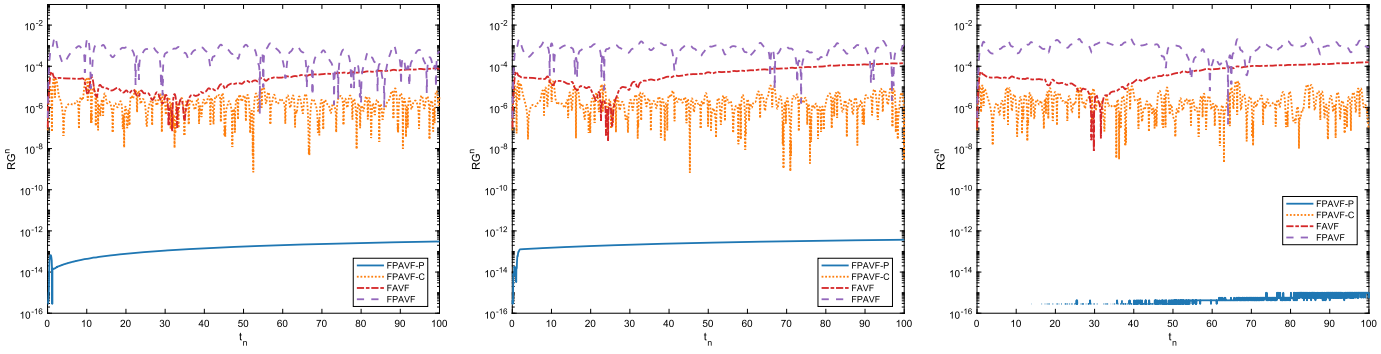

(a) $\alpha = 1.3$ (b) $\alpha = 1.6$ (c) $\alpha = 1.9$

Fig. 11. The relative errors of discrete mass for different α in Example 4.2 with $N = 64$ and $\tau = 0.01$.

affect the shape of the waves, and the shape of the wave changes faster when α becomes larger. Specifically, the numerical solutions converge to the classical nonlinear Schrödinger wave equation when $\alpha \to 2$, see [4,32,33].

5. Conclusions and remarks

In this paper, we reformulate the two-dimensional fractional nonlinear Schrödinger wave equations as a canonical Hamiltonian system.

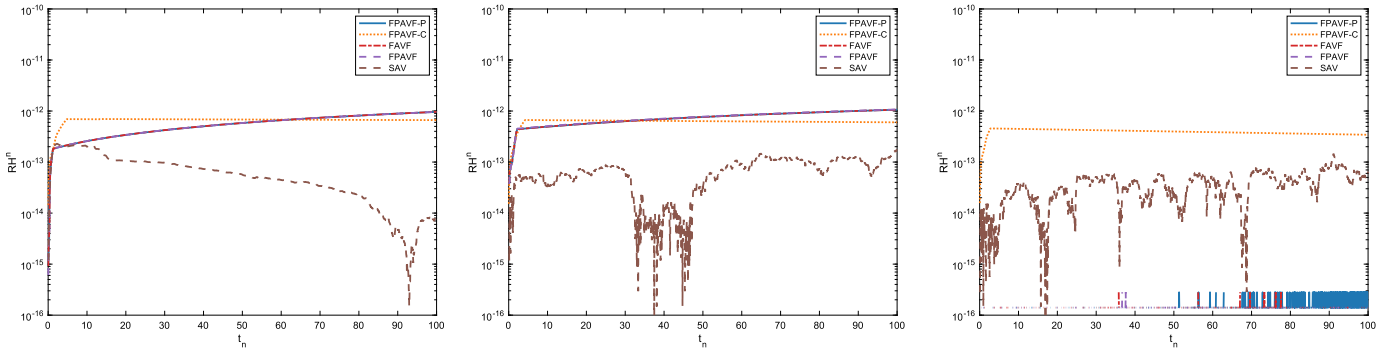

(a) $\alpha = 1.3$ (b) $\alpha = 1.6$ (c) $\alpha = 1.9$

Fig. 12. The relative errors of discrete energy for different α in Example 4.2 with $N = 64$ and $\tau = 0.01$.

Table 6
Discrete mass G^n at time $t = t_n$ for Example 4.2 when $\alpha = 1.3$.

t	FAVF	FPAVF	FPAVF-C	FPAVF-P
0	3.14159297667455	3.14159361842152	3.14159241227909	3.14159265358976
10	3.14160952253933	3.13595374862870	3.14166505643569	3.14159265358963
20	3.14161343543099	3.14421089321261	3.14158965037808	3.14159265358952
40	3.14157539023564	3.14362067013654	3.14159917106759	3.14159265358932
60	3.14150249358846	3.14217508702013	3.14159868539556	3.14159265358912
80	3.14143174175214	3.14159826267015	3.14158946625201	3.14159265358895
100	3.14135672071641	3.14328710863969	3.14158227319751	3.14159265358880
				Original mass: 3.14159265323701

Table 7
Discrete mass G^n at time $t = t_n$ for Example 4.2 when $\alpha = 1.6$.

t	FAVF	FPAVF	FPAVF-C	FPAVF-P
0	3.14159297668940	3.14159361814729	3.14159241218683	3.14159265358976
10	3.14163389358031	3.13754191888209	3.14160072631792	3.14159265358928
20	3.14161716177523	3.14433222488425	3.14159044899067	3.14159265358919
40	3.14149554093894	3.14475213344308	3.14160500647197	3.14159265358901
60	3.14139997924855	3.14288256207779	3.14160023436812	3.14159265358885
80	3.14127488637752	3.14241392600216	3.14158768432513	3.14159265358871
100	3.14115287766347	3.14489331385338	3.14159412822417	3.14159265358860
				Original mass: 3.14159265323701

Table 8
Discrete mass G^n at time $t = t_n$ for Example 4.2 when $\alpha = 2$.

t	FAVF	FPAVF	FPAVF-C	FPAVF-P
0	3.14159297725470	3.14159361919902	3.14159241149324	3.14159265358976
10	3.14168000260412	3.14369215006721	3.14160070161208	3.14159265358976
20	3.14164544531849	3.14521250122401	3.14158745249453	3.14159265358976
40	3.14150535695500	3.14531702832209	3.14160031804829	3.14159265358976
60	3.14136438511727	3.14552013864766	3.14159560564481	3.14159265358976
80	3.14118013227991	3.14739329967543	3.14158800109644	3.14159265358976
100	3.14101125059928	3.15011874273391	3.14154787019595	3.14159265358976
				Original mass: 3.14159265323701

By combining the partitioned averaged vector field plus method and Fourier pseudo-spectral method, we construct a conservative numerical scheme based on the resulting Hamiltonian system. Theoretical analysis and numerical findings reveal that the proposed method can preserve the original energy and mass effectively.

Data availability

Data will be made available on request.

Acknowledgements

This work is supported by the Sichuan Science and Technology Program (Grant No. 2022JDTD0019) and the National-Local Joint Engineering Laboratory of System Credibility Automatic Verification (Grant No. ZD20220105).

References

[1] L. Caffarelli, L. Silvestre, An extension problem related to the fractional Laplacian, Commun. Partial Differ. Equ. 32 (8) (2007) 1245–1260.
[2] Q. Yang, F. Liu, I. Turner, Numerical methods for fractional partial differential equations with Riesz space fractional derivatives, Appl. Math. Model. 34 (1) (2010) 200–218.
[3] F. Demengel, G. Demengel, Functional Spaces for the Theory of Elliptic Partial Differential Equations, Universitext, Springer, London, 2012.
[4] L. Zhang, Q. Chang, A conservative numerical scheme for a class of nonlinear Schrödinger equation with wave operator, Appl. Math. Comput. 145 (2) (2003) 603–612.

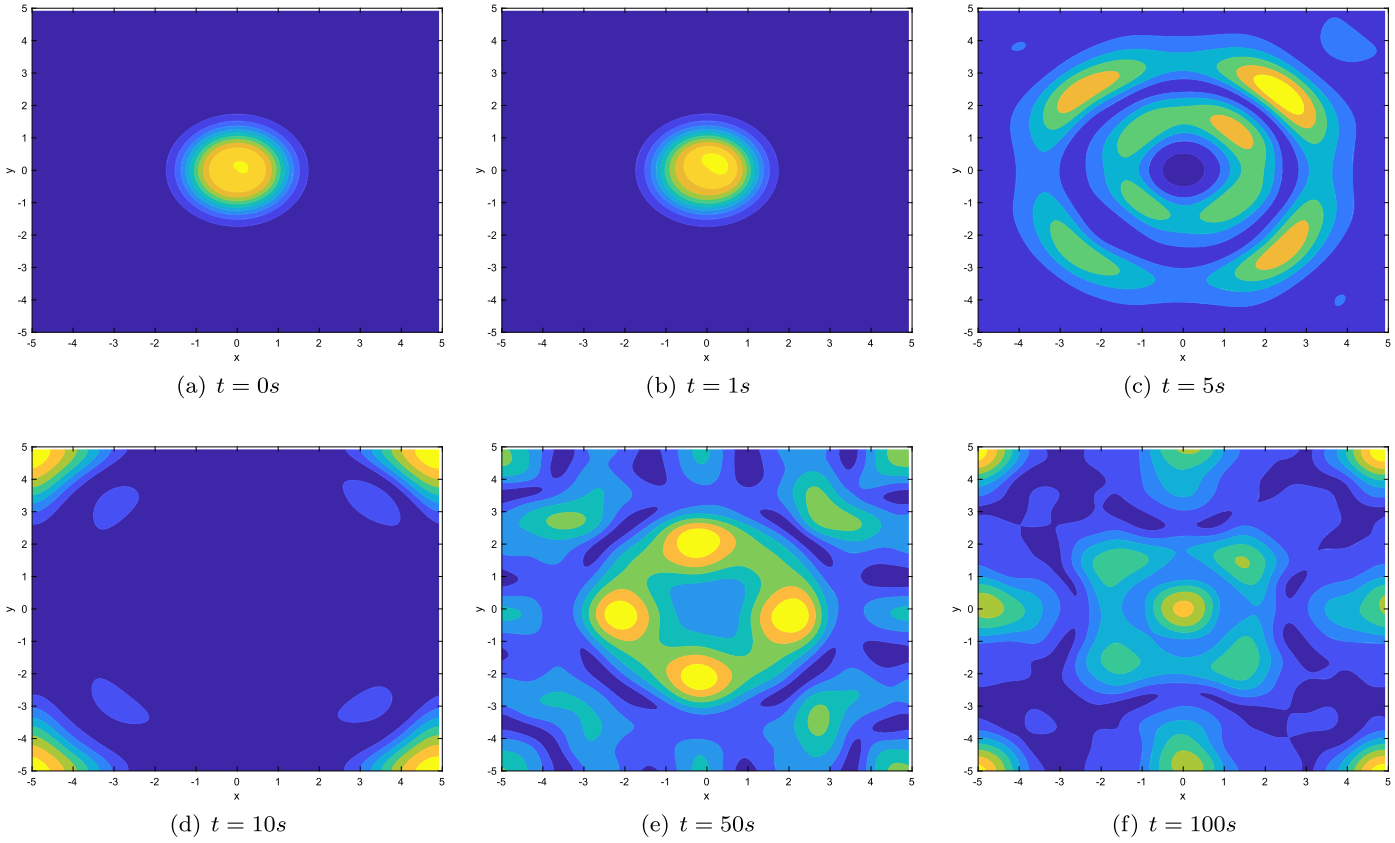

Fig. 13. The pictures of wave propagation for Example 4.2 with $\alpha = 1.3$.

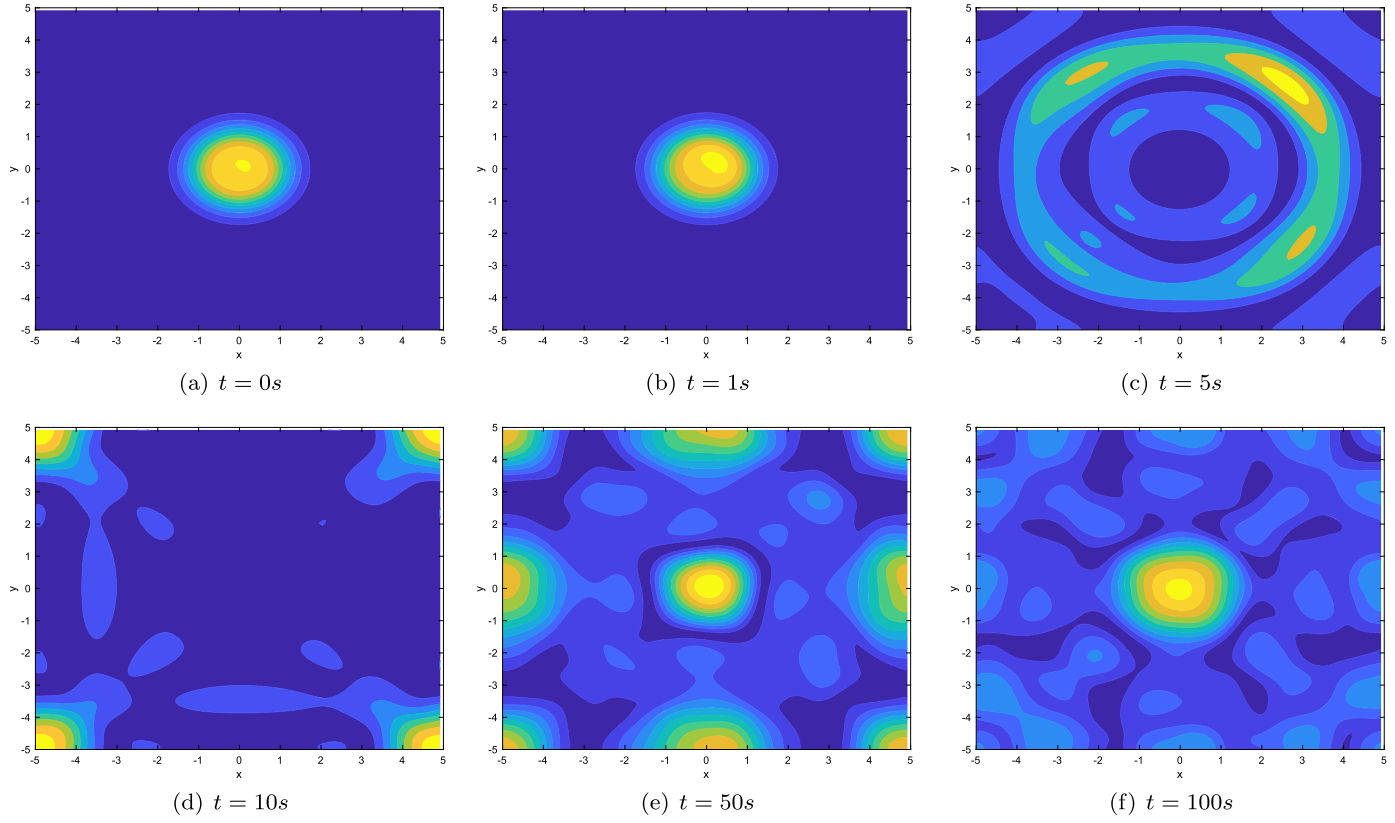

Fig. 14. The pictures of wave propagation for Example 4.2 with $\alpha = 1.6$.

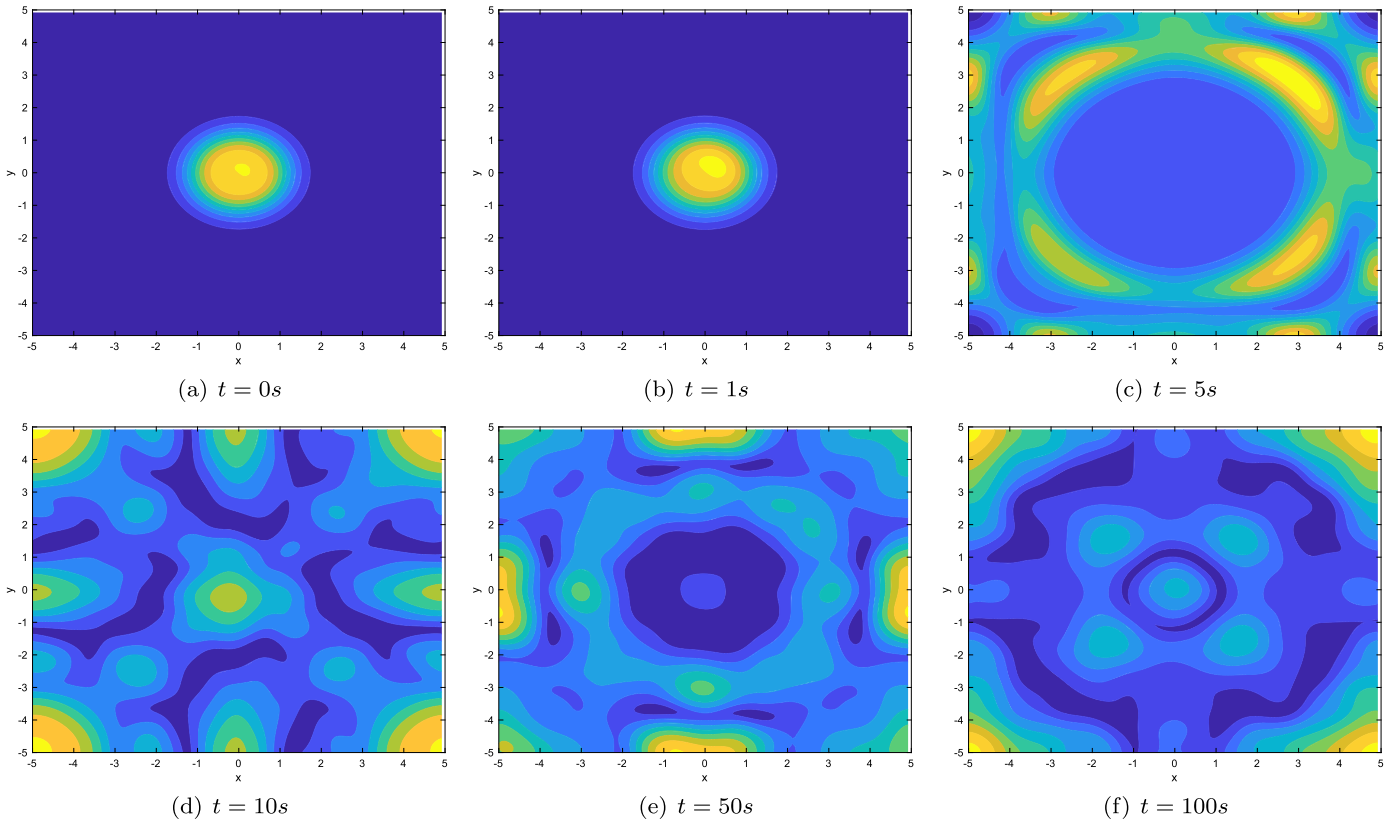

Fig. 15. The pictures of wave propagation for Example 4.2 with $\alpha = 1.99$.

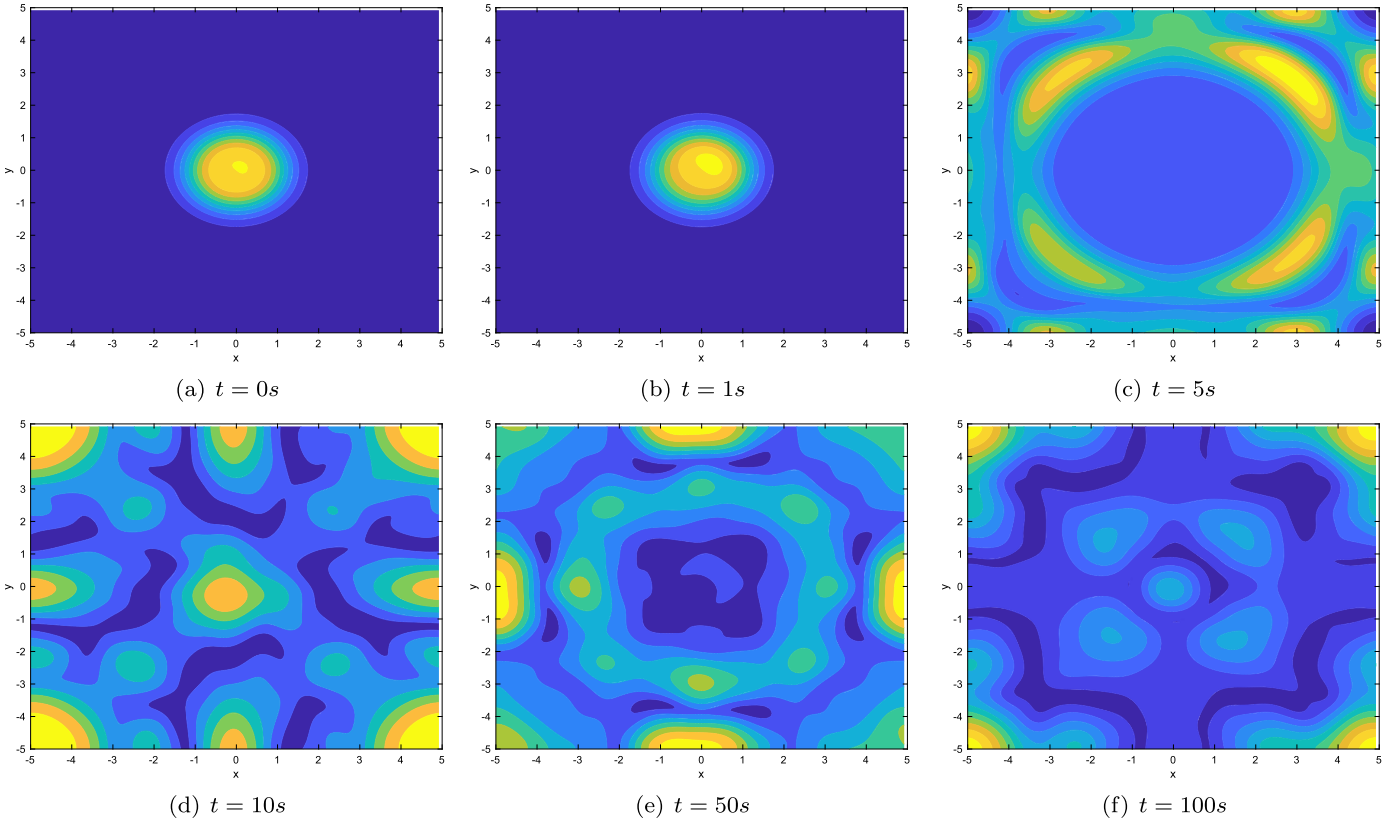

Fig. 16. The pictures of wave propagation for Example 4.2 with $\alpha = 2$.

[5] W. Bao, Y. Cai, Error estimates of finite difference methods for the nonlinear Schrödinger equation with wave operator, SIAM J. Numer. Anal. 50 (2) (2012) 492–521.
[6] X. Cheng, F. Wu, Several conservative compact schemes for a class of nonlinear Schrödinger equations with wave operator, Bound. Value Probl. 2018 (1) (2018) 40.
[7] L. Brugnano, C. Zhang, D. Li, A class of energy-conserving Hamiltonian boundary value methods for nonlinear Schrödinger equation with wave operator, Commun. Nonlinear Sci. Numer. Simul. 60 (2018) 33–49.
[8] M. Tsutsumi, Nonrelativistic approximation of nonlinear Klein-Gordon equations in two space dimensions, Nonlinear Anal., Theory Methods Appl. 8 (6) (1984) 637–643.
[9] S. Machihara, K. Nakanishi, T. Ozawa, Nonrelativistic limit in the energy space for nonlinear Klein-Gordon equations, Math. Ann. 322 (3) (2002) 603–621.
[10] T. Colin, P. Fabrie, Semidiscretization in time for nonlinear Schrödinger-waves equations, Discrete Contin. Dyn. Syst. 4 (4) (Tue Jun 30 20:00:00 EDT 1998) 671–690.
[11] W. Bao, X. Dong, J. Xin, Comparisons between sine-Gordon and perturbed nonlinear Schrödinger equations for modeling light bullets beyond critical collapse, Phys. D, Nonlinear Phenom. 239 (13) (2010) 1120–1134.
[12] J. Xin, Modeling light bullets with the two-dimensional sine-Gordon equation, Phys. D, Nonlinear Phenom. 135 (3–4) (2000) 345–368.
[13] N. Laskin, Fractional quantum mechanics, Phys. Rev. E 62 (3) (2000) 3135–3145.
[14] N. Laskin, Fractional Schrodinger equation, Phys. Rev. E 66 (5) (2002) 056108.
[15] S. Li, L. Vu-Quoc, Finite difference calculus invariant structure of a class of algorithms for the nonlinear Klein-Gordon equation, SIAM J. Numer. Anal. 32 (6) (1995) 1839–1875.
[16] D. Wang, A. Xiao, W. Yang, Crank-Nicolson difference scheme for the coupled nonlinear Schrödinger equations with the Riesz space fractional derivative, J. Comput. Phys. 242 (2013) 670–681.
[17] D. Wang, A. Xiao, W. Yang, A linearly implicit conservative difference scheme for the space fractional coupled nonlinear Schrödinger equations, J. Comput. Phys. 272 (2014) 644–655.
[18] M. Ran, C. Zhang, A conservative difference scheme for solving the strongly coupled nonlinear fractional Schrödinger equations, Commun. Nonlinear Sci. Numer. Simul. 41 (2016) 64–83.
[19] P. Wang, C. Huang, An energy conservative difference scheme for the nonlinear fractional Schrödinger equations, J. Comput. Phys. 293 (2015) 238–251.
[20] P. Wang, C. Huang, A conservative linearized difference scheme for the nonlinear fractional Schrödinger equation, Numer. Algorithms 69 (3) (2015) 625–641.
[21] Y. Wang, L. Mei, Q. Li, L. Bu, Split-step spectral Galerkin method for the two-dimensional nonlinear space-fractional Schrödinger equation, Appl. Numer. Math. 136 (2019) 257–278.
[22] M. Ran, C. Zhang, A linearly implicit conservative scheme for the fractional nonlinear Schrödinger equation with wave operator, Int. J. Comput. Math. 93 (7) (2016) 1103–1118.
[23] M. Li, Y.-L. Zhao, A fast energy conserving finite element method for the nonlinear fractional Schrödinger equation with wave operator, Appl. Math. Comput. 338 (2018) 758–773.
[24] X. Cheng, H. Qin, J. Zhang, Convergence of an energy-conserving scheme for nonlinear space fractional Schrödinger equations with wave operator, J. Comput. Appl. Math. 400 (2022) 113762.
[25] D. Hu, W. Cai, X.-M. Gu, Y. Wang, Efficient energy preserving Galerkin-Legendre spectral methods for fractional nonlinear Schrödinger equation with wave operator, Appl. Numer. Math. 172 (2022) 608–628.
[26] X. Zhang, M. Ran, Y. Liu, L. Zhang, A high-order structure-preserving difference scheme for generalized fractional Schrödinger equation with wave operator, Math. Comput. Simul. 210 (2023) 532–546.
[27] C. Budd, A. Iserles, R.I. McLachlan, G.R.W. Quispel, N. Robidoux, Geometric integration using discrete gradients, Philos. Trans. R. Soc. Lond. A, Math. Phys. Eng. Sci. 357 (1754) (1999) 1021–1045.
[28] G.R.W. Quispel, D.I. McLaren, A new class of energy-preserving numerical integration methods, J. Phys. A, Math. Theor. 41 (4) (2008) 045206.
[29] W. Cai, H. Li, Y. Wang, Partitioned averaged vector field methods, J. Comput. Phys. 370 (2018) 25–42.
[30] P. Wang, C. Huang, Structure-preserving numerical methods for the fractional Schrödinger equation, Appl. Numer. Math. 129 (2018) 137–158.
[31] Y. Fu, W. Cai, Y. Wang, Structure-preserving algorithms for the two-dimensional fractional Klein-Gordon-Schrödinger equation, Appl. Numer. Math. 156 (2020) 77–93.
[32] X. Li, L. Zhang, S. Wang, A compact finite difference scheme for the nonlinear Schrödinger equation with wave operator, Appl. Math. Comput. 219 (6) (2012) 3187–3197.
[33] T.-C. Wang, L.-M. Zhang, Analysis of some new conservative schemes for nonlinear Schrödinger equation with wave operator, Appl. Math. Comput. 182 (2) (2006) 1780–1794.